symmetry

IMPACT FACTOR 2.2

CITESCORE 5.4

Article

Triply Heavy Tetraquark States in a Mass-Splitting Model

Shi-Yuan Li, Yan-Rui Liu, Zi-Long Man, Cheng-Rui Shu, Zong-Guo Si and Jing Wu

Special Issue
Symmetry in Hadron Physics

Edited by
Prof. Dr. Jialun Ping

MDPI

https://doi.org/10.3390/sym17020170

symmetry

MDPI

Article

Triply Heavy Tetraquark States in a Mass-Splitting Model

Shi-Yuan Li [1], Yan-Rui Liu [1,*], Zi-Long Man [2,3,4,5,6,*], Cheng-Rui Shu [1], Zong-Guo Si [1] and Jing Wu [7,*]

[1] School of Physics, Shandong University, Jinan 250100, China
[2] School of Physical Science and Technology, Lanzhou University, Lanzhou 730000, China
[3] Lanzhou Center for Theoretical Physics, Lanzhou University, Lanzhou 730000, China
[4] Key Laboratory of Quantum Theory and Applications of MoE, Lanzhou University, Lanzhou 730000, China
[5] Key Laboratory of Theoretical Physics of Gansu Province, Lanzhou University, Lanzhou 730000, China
[6] Research Center for Hadron and CSR Physics, Lanzhou University and Institute of Modern Physics of CAS, Lanzhou 730000, China
[7] School of Science, Shandong Jianzhu University, Jinan 250101, China
* Correspondence: yrliu@sdu.edu.cn (Y.-R.L.); manzl@lzu.edu.cn (Z.-L.M.); wujing18@sdjzu.edu.cn (J.W.)

Abstract: In a modified chromomagnetic interaction model, assuming $X(4140)$ to be the lowest 1^{++} $cs\bar{c}\bar{s}$ tetraquark and treating it as the reference state, we systematically investigated the masses of the triply heavy tetraquark states $QQ\bar{Q}\bar{q}$ ($Q = c, b; q = u, d, s$). Because of their higher masses, no stable tetraquarks were found. Using a simple scheme, we also estimated the partial widths of the rearrangement decay channels and relevant ratios. A compact triply heavy tetraquark candidate would be favored if its observed mass and partial width ratios were comparable with our predictions. We hope that the present work will be helpful for further studies.

Keywords: tetraquark; chromomagnetic interaction; spectrum; decay

Academic Editor: Jorge Segovia

Received: 23 December 2024
Revised: 10 January 2025
Accepted: 14 January 2025
Published: 23 January 2025

Citation: Li, S.-Y.; Liu, Y.-R.; Man, Z.-L.; Shu, C.-R.; Si, Z.-G.; Wu, J. Triply Heavy Tetraquark States in a Mass-Splitting Model. *Symmetry* **2025**, *17*, 170. https://doi.org/10.3390/sym17020170

1. Introduction

Since the observation of the exotic $X(3872)$ by the Belle Collaboration in 2003 [1], tens of charmonium-like and bottomonium-like states with the names X, Y, or Z have been identified over the past two decades [2–12]. In particular, charged charmonium-like or bottomonium-like states were found, such as $Z_c(3900)$ [13–16], $Z_c(3885)$ [17,18], $Z_c(4020)$ [19,20], $Z_c(4025)$ [21,22], $Z_{cs}(3985)$ [23], $Z_{cs}(4000)$ [24], $Z_{cs}(4220)$ [24], $Z_b(10{,}610)$ [25], and $Z_b(10{,}650)$ [25], which cannot be classified as excited heavy quarkonia and are explicitly exotic. Their properties may be understood in configurations such as the compact tetraquark [26–28] and the meson–antimeson molecule [29–32]. In 2020, the LHCb Collaboration observed a broad structure that ranged from 6.2 to 6.8 GeV and a narrow one located around 6.9 GeV in the $J/\psi J/\psi$ channel, while the latter was called $X(6900)$ [33]. They are good candidates for fully heavy tetraquark states. More candidates were announced in [34–36]. It is essential to study the exotic structures from broader and deeper perspectives [37–47].

In addition to the hidden heavy case, open heavy exotics have been observed in recent years. In 2016, the D0 Collaboration reported the observation of the singly bottom $X(5568)$ in the $B_s^0\pi^\pm$ channel [48]. This four-quark state is about 200 MeV below the $B\bar{K}$ threshold. However, the LHCb Collaboration [49] and the CMS Collaboration did not corroborate the presence of this state, casting doubt on its existence. In 2020, the LHCb observed an exotic peak in the D^-K^+ channel [50,51]. To fit the experimental data, the collaboration introduced two resonances named $T_{cs0}(2900)^0$ ($J = 0$) and $T_{cs1}(2900)^0$ ($J = 1$), whose minimal quark content is $ud\bar{s}\bar{c}$. In 2023, they observed another two singly charm tetraquark

states: $T^a_{c\bar{s}0}(2900)^0$ and $T^a_{c\bar{s}0}(2900)^{++}$ [52,53]. In the double-charm case, the LHCb also produced a new finding. In 2021, they reported the observation of a narrow state named $T^+_{cc}(3875)$ in the $D^0D^0\pi^+$ mass spectrum, just below the $D^{*+}D^0$ threshold [54,55]. This state has a minimal quark content of $cc\bar{u}\bar{d}$ and is a good candidate for the theoretically anticipated double-charm tetraquark T_{cc} [45].

Until now, possible singly, doubly, and fully charm tetraquark states have been observed. The existence of triply heavy tetraquarks is also possible. Distinguishing between compact states and hadronic molecules is often challenging for researchers. However, in the case of the fully heavy-state $QQ\bar{Q}\bar{Q}$ ($Q = c, b$), the meson exchange interaction may be suppressed, while the short-range one-gluon exchange interaction should play a dominant role in the binding force. It is very likely that the observed $X(6900)$ is a compact tetraquark. The situation is similar for the triply heavy $QQ\bar{Q}\bar{q}$ ($q = u, d, s$) states. If such a state were observed in future experiments, understanding its properties in a compact picture is highly feasible. The authors of [56,57] considered the possibility of fully heavy four-quark molecular states using heavy meson exchange forces. If such interactions do play an important role, triply heavy four-quark molecular states should also be possible.

To date, there have been several theoretical explorations of triply heavy tetraquark states using various methods. With the assumption that the input $X(3872)$ is a tetraquark state, triply heavy tetraquark spectra were studied in [58] using a chromomagnetic interaction (CMI) model, and some stable states were found. A different CMI model adopted in [59] also gave some stable states. However, unstable states were obtained with an extended CMI model in [60]. From calculations utilizing lattice QCD [61,62], shallow bound $uc\bar{b}\bar{b}$ and $sc\bar{b}\bar{b}$ states are possible. A study that used the QCD sum rule [63] indicated that narrow resonances are possible, while a recent calculation [64] gave heavier $cc\bar{c}\bar{q}/bb\bar{b}\bar{q}$ ($q = u, d, s$) states. Nonstrange multiquarks, as compact topological molecules, were studied using a holographic approach in [65], which revealed that the $QQ\bar{Q}\bar{q}$ states are unbound. Stable candidates were obtained in the $cc\bar{c}\bar{n}$ sector using an AdS/QCD potential model [66]. Using the MIT bag model, ref. [67] indicated that all the triply heavy tetraquarks are above the corresponding meson–meson thresholds. The authors of [68] also drew the conclusion that there are no stable $QQ\bar{Q}\bar{q}$ states by employing an extended relativized quark model. A similar conclusion was obtained in [69], where pure and chiral constituent quark models were employed. With their constituent quark models, the authors of [70,71] found that bound $cc\bar{c}\bar{n}$ states are possible when coupled channel effects are considered. In addition to mass calculations, the authors of [72] employed two models, namely, the effective Hamiltonian in the diquark–antidiquark picture and the nonrelativistic quark model, to study the decay properties of $bb\bar{c}\bar{n}$ ($n = u, d$) states.

When determining the spectra of triply heavy tetraquark states with a CMI model, in [59], we utilized meson–meson thresholds as reference scales. Several states below the corresponding lowest meson–meson thresholds were found, which indicates that they may be stable; e.g., the lowest 1^+ $cc\bar{b}\bar{n}$ was below the B_cD^* threshold. However, the obtained tetraquark masses may have been underestimated [59,73,74]. To reduce the estimation uncertainty, following the study method for tetraquarks adopted in [73–76], we reconsidered the $QQ\bar{Q}\bar{q}$ ($q = u, d, s$) spectra by treating 1^{++} $X(4140)$ [6,7] as the reference tetraquark state. Since the inner structures between the meson–meson and compact states are different, the masses estimated using this method should be more reasonable. We also discussed the two-body rearrangement decays, which were not considered in [59], by employing a simple scheme.

This paper is organized as follows: In Section 2, we present the formalism containing the mass formulae, color–spin base vectors, CMI matrices for different systems, and scheme to study the rearrangement decays. In Section 3, we collect the parameters for the calcula-

tion and the numerical results, including the spectra and rearrangement decay widths. We provide a discussion and a short summary in the last section.

2. Formalism

2.1. Spectrum Calculation

In this work, we employed the CMI model to study the S-wave triply heavy tetraquark states. The model Hamiltonian reads as

$$H = \sum_i m_i + H_{CMI} = \sum_i m_i - \sum_{i<j} C_{ij} \lambda_i \cdot \lambda_j \sigma_i \cdot \sigma_j. \quad (1)$$

Here, m_i is the effective mass of the ith quark component, which contains contributions from the kinetic energy, color–Coulomb potential, and color confinement. The effective parameter C_{ij} reflects the coupling strength between the ith and jth quark components. λ_i and σ_i are the Gell–Mann and Pauli matrices, respectively, for the ith quark. For antiquarks, λ_i should be replaced with $-\lambda_i^*$. The chromomagnetic term H_{CMI} induces mass splittings for the tetraquark states. With the constructed color–spin base vectors, the CMI matrix $\langle H_{CMI} \rangle$ can be obtained; diagonalizing it gives the mass formula for a compact tetraquark:

$$M = \sum_i m_i + E_{CMI}, \quad (2)$$

where E_{CMI} indicates the eigenvalue of $\langle H_{CMI} \rangle$ corresponding to this state.

Since the effective quark masses are extracted from the spectra of conventional mesons and baryons, they may not be suitable for tetraquark states. From previous studies [45,73–76], we found that the values calculated using Equation (2) tend to be larger than the possible tetraquark masses. This discrepancy is primarily attributed to the values of effective quark masses, which may not accurately reflect the interactions within tetraquark states. Each hadron has quark masses tailored to its specific structure, and the extracted values may not be directly applicable to multiquark systems. The overestimated tetraquark masses from Equation (2) are regarded as the theoretical upper limits in the following discussions.

To reduce the uncertainties and obtain more reasonable tetraquark spectra, one may adopt a modified mass formula by introducing a reference state that has the same quark content as the studied tetraquark:

$$M = [M_{ref} - (E_{CMI})_{ref}] + E_{CMI}. \quad (3)$$

Here, M_{ref} and $(E_{CMI})_{ref}$ denote the measured mass and the calculated CMI eigenvalue for the reference state, respectively. One of the choices for the reference scale M_{ref} for a considered system is a meson–meson threshold. However, previous studies [59,73,74] indicated that such a choice is not unique and may result in tetraquark masses lower than the measured values. The reason should be that interactions between constituent quarks in compact multiquark states are complex and cannot be fully reflected in a simple hadron–hadron state. We regard the underestimated tetraquark masses from Equation (3) as the theoretical lower limits in the following.

To obtain more reasonable values, it is necessary to choose a reference scale for all tetraquark mass estimations. Considering that the dynamics of two tetraquark states are comparable, it is reasonable to select a tetraquark candidate to determine the scale. In previous studies [73–76], we treated $X(4140)$ as the reference by assuming it to be the lowest 1^{++} compact $cs\bar{c}\bar{s}$ state. In this work, we again adopted this assumption. The considerations were as follows: First, $X(4140)$ as a $J/\psi\phi$ resonance was confirmed by

different experiments with the determined quantum numbers $J^{PC} = 1^{++}$. Second, the exotic state $X(4274)$ was observed in the $J/\psi\phi$ channel by CDF and LHCb [24,77] with the same quantum numbers as $X(4140)$. These states can be interpreted consistently as partner states in the compact $cs\bar{c}\bar{s}$ picture [78,79]. Additionally, from discussions on the reference state selection problem in [75], we found that adopting $X(4140)$ as the reference can give more reasonable interpretations for other $cs\bar{c}\bar{s}$ states. Now, a second modified mass formula reads as

$$\begin{aligned} M &= M_{X(4140)} - (E_{CMI})_{X(4140)} + E_{CMI} + \sum_{ij} n_{ij}(m_i - m_j) \\ &= \tilde{m} + E_{CMI} + \sum_{ij} n_{ij}\Delta_{ij}. \end{aligned} \tag{4}$$

Here, $M_{X(4140)}$ and $(E_{CMI})_{X(4140)}$ are the measured mass and calculated CMI eigenvalue of $X(4140)$, respectively. The quark contents are different for triply heavy tetraquarks and the hidden-charm $X(4140)$. This modified formula means that we used the quark mass gap $\Delta_{ij} = m_i - m_j$ rather than the quark masses themselves, as well as the integer number n_{ij} to parameterize the scale difference. The value of Δ_{ij} was extracted from the conventional hadron masses. Explicitly, the mass formulae for the systems considered in this study were

$$\begin{aligned} M_{cc\bar{c}\bar{n}} &= \tilde{m} + \langle H_{CMI}\rangle + \Delta_{cs} - \Delta_{sn}, \\ M_{cc\bar{c}\bar{s}} &= \tilde{m} + \langle H_{CMI}\rangle + \Delta_{cs}, \\ M_{cc\bar{b}\bar{n}} &= \tilde{m} + \langle H_{CMI}\rangle + \Delta_{bs} - \Delta_{sn}, \\ M_{cc\bar{b}\bar{s}} &= \tilde{m} + \langle H_{CMI}\rangle + \Delta_{bs}, \\ M_{bb\bar{c}\bar{n}} &= \tilde{m} + \langle H_{CMI}\rangle + 2\Delta_{bs} - \Delta_{cn}, \\ M_{bb\bar{c}\bar{s}} &= \tilde{m} + \langle H_{CMI}\rangle + \Delta_{bc} + \Delta_{bs}, \\ M_{bb\bar{b}\bar{n}} &= \tilde{m} + \langle H_{CMI}\rangle + 2\Delta_{bs} + \Delta_{bc} - \Delta_{cn}, \\ M_{bb\bar{b}\bar{s}} &= \tilde{m} + \langle H_{CMI}\rangle + 2\Delta_{bc} + \Delta_{bs}, \\ M_{bc\bar{c}\bar{n}} &= M_{cc\bar{b}\bar{n}}, \quad M_{bc\bar{c}\bar{s}} = M_{cc\bar{b}\bar{s}}, \\ M_{bc\bar{b}\bar{n}} &= M_{bb\bar{c}\bar{n}}, \quad M_{bc\bar{b}\bar{s}} = M_{bb\bar{c}\bar{s}}. \end{aligned} \tag{5}$$

Although the formulae for different systems may have been the same, the number of states and the mass spectra were not. We discuss the results calculated with these formulae.

2.2. Color–Spin Base Vectors and CMI Hamiltonians

It is essential to establish color $\otimes$ spin base vectors to obtain the CMI matrices. We chose the diquark–antidiquark configuration to describe the bases. They were the same as those in [59]:

$$\begin{aligned} \phi_1\chi_1 &= |(Q_1Q_2)_1^6(\bar{Q}_3\bar{q}_4)_1^{\bar{6}}\rangle_2\delta_{12}, \\ \phi_1\chi_2 &= |(Q_1Q_2)_1^6(\bar{Q}_3\bar{q}_4)_1^{\bar{6}}\rangle_1\delta_{12}, \\ \phi_1\chi_3 &= |(Q_1Q_2)_1^6(\bar{Q}_3\bar{q}_4)_1^{\bar{6}}\rangle_0\delta_{12}, \\ \phi_1\chi_4 &= |(Q_1Q_2)_1^6(\bar{Q}_3\bar{q}_4)_0^{\bar{6}}\rangle_1\delta_{12}, \\ \phi_1\chi_5 &= |(Q_1Q_2)_0^6(\bar{Q}_3\bar{q}_4)_1^{\bar{6}}\rangle_1, \\ \phi_1\chi_6 &= |(Q_1Q_2)_0^6(\bar{Q}_3\bar{q}_4)_0^{\bar{6}}\rangle_0, \\ \phi_2\chi_1 &= |(Q_1Q_2)_1^{\bar{3}}(\bar{Q}_3\bar{q}_4)_1^{3}\rangle_2, \\ \phi_2\chi_2 &= |(Q_1Q_2)_1^{\bar{3}}(\bar{Q}_3\bar{q}_4)_1^{3}\rangle_1, \\ \phi_2\chi_3 &= |(Q_1Q_2)_1^{\bar{3}}(\bar{Q}_3\bar{q}_4)_1^{3}\rangle_0, \\ \phi_2\chi_4 &= |(Q_1Q_2)_1^{\bar{3}}(\bar{Q}_3\bar{q}_4)_0^{3}\rangle_1, \\ \phi_2\chi_5 &= |(Q_1Q_2)_0^{\bar{3}}(\bar{Q}_3\bar{q}_4)_1^{3}\rangle_1\delta_{12}, \\ \phi_2\chi_6 &= |(Q_1Q_2)_0^{\bar{3}}(\bar{Q}_3\bar{q}_4)_0^{3}\rangle_0\delta_{12}, \end{aligned} \tag{6}$$

where ϕ and χ are color and spin base vectors, respectively, and the notation on the right-hand side is $|(Q_1Q_2)^{color}_{spin}(\bar{Q}_3\bar{q}_4)^{color}_{spin}\rangle_{spin}$. The δ_{12} symbol arises from the Pauli principle. It is set to 0 if Q_1 and Q_2 are identical; otherwise, it is equal to 1. This convention means that the corresponding base vector does not exist for states with $Q_1 = Q_2$. Therefore, we could categorize the studied systems into two groups: one contained $cc\bar{Q}\bar{q}$ and $bb\bar{Q}\bar{q}$ systems, and the other contained $bc\bar{Q}\bar{q}$. The first group involved six base vectors, but all twelve bases were involved in the second group.

To express the matrices succinctly, here, we define $\alpha = C_{12} + C_{34}$, $\gamma = C_{12} - C_{34}$, $\beta = C_{13} + C_{14} + C_{23} + C_{24}$, $\delta = C_{13} - C_{14} + C_{23} - C_{24}$, $\mu = C_{13} - C_{14} - C_{23} + C_{24}$, and $\nu = C_{13} + C_{14} - C_{23} - C_{24}$. For the 2^+, 1^+, and 0^+ states in the first group, the corresponding CMI matrices were $\frac{4}{3}(2\alpha + \beta)$ with the base vector $(\phi_2\chi_1)^T$,

$$\begin{pmatrix} \frac{4}{3}(2\alpha - \beta) & \frac{4}{3}\sqrt{2}\delta & 4\delta \\ & \frac{8}{3}(2\gamma - \alpha) & -2\sqrt{2}\beta \\ & & \frac{4}{3}(\alpha + 2\gamma) \end{pmatrix} \tag{7}$$

with the base vector $(\phi_2\chi_2, \phi_2\chi_4, \phi_1\chi_5)^T$, and

$$\begin{pmatrix} \frac{8}{3}(\alpha - \beta) & 2\sqrt{6}\beta \\ & 4\alpha \end{pmatrix} \tag{8}$$

with the base vector $(\phi_2\chi_3, \phi_1\chi_6)^T$. For the 2^+, 1^+, and 0^+ states in the second group, the corresponding CMI matrices were

$$\begin{pmatrix} -\frac{4}{3}\alpha + \frac{10}{3}\beta & -2\sqrt{2}\mu \\ & \frac{4}{3}(2\alpha + \beta) \end{pmatrix}, \tag{9}$$

$$\begin{pmatrix} -\frac{4}{3}\alpha - \frac{10}{3}\beta & \frac{10}{3}\sqrt{2}\delta & -\frac{10}{3}\sqrt{2}\nu & 2\sqrt{2}\mu & -4\nu & 4\delta \\ & \frac{4}{3}(\alpha - 2\gamma) & \frac{10}{3}\mu & -4\nu & 0 & -2\sqrt{2}\beta \\ & & \frac{4}{3}(\alpha + 2\gamma) & 4\delta & -2\sqrt{2}\beta & 0 \\ & & & \frac{4}{3}(2\alpha - \beta) & \frac{4}{3}\sqrt{2}\delta & -\frac{4}{3}\sqrt{2}\nu \\ & & & & \frac{8}{3}(2\gamma - \alpha) & \frac{4}{3}\mu \\ & & & & & -\frac{8}{3}(\alpha + 2\gamma) \end{pmatrix}, \tag{10}$$

and

$$\begin{pmatrix} \frac{8}{3}(\alpha - \beta) & -\frac{4}{3}\sqrt{3}\mu & 4\sqrt{2}\mu & 2\sqrt{6}\beta \\ & -8\alpha & 2\sqrt{6}\beta & 0 \\ & & -\frac{4}{3}(\alpha + 5\beta) & -\frac{10}{3}\sqrt{3}\mu \\ & & & 4\alpha \end{pmatrix}. \tag{11}$$

Their base vectors were $(\phi_1\chi_1, \phi_2\chi_1)^T$, $(\phi_1\chi_2, \phi_1\chi_4, \phi_1\chi_5, \phi_2\chi_2, \phi_2\chi_4, \phi_2\chi_5)^T$, and $(\phi_2\chi_3, \phi_2\chi_6, \phi_1\chi_3, \phi_1\chi_6)^T$, respectively. Since each CMI matrix was symmetric, here, we only write down the upper triangular part.

2.3. Rearrangement Decay

Our study also involved the rearrangement decays, which were found to be helpful in understanding exotic hadron structures by combining information from spectra and decay widths [73,75,80,81]. The simple scheme that we adopted was just to estimate the scattering amplitude $\mathcal{M}$ by taking the decay Hamiltonian as a constant $H_{decay} = \mathcal{C}$. Then,

the amplitude was written as $\mathcal{M} = \langle final|H_{decay}|initial\rangle = \mathcal{C}\langle final|initial\rangle$, and the decay width was

$$\Gamma = |\mathcal{M}|^2 \frac{|\vec{p}|}{8\pi M^2}, \tag{12}$$

where M is the initial tetraquark state mass, and $\vec{p}$ is the three-momentum of a final meson in the center-of-mass frame. To obtain the $\mathcal{M}$ values, we needed the flavor–color–spin wave functions of $|initial\rangle$ and $|final\rangle$. The final state had two possible configurations: $(Q_1\bar{Q}_3)^{1c}(Q_2\bar{q}_4)^{1c}$ and $(Q_1\bar{q}_4)^{1c}(Q_2\bar{Q}_3)^{1c}$. They could be expressed as superpositions of the base vectors given in the last subsection with different coefficients. Supposing that $|initial\rangle = \sum_{i=1}^{12} x_i\psi_i$ and $|final\rangle = \sum_{i=1}^{12} y_i\psi_i$, where ψ_i is the ith base vector, we obtained $\mathcal{M} = \mathcal{C}\sum_{i=1}^{12} x_i y_i$ and Γ immediately.

3. Spectra and Widths of Triply Heavy Tetraquarks

3.1. Model Parameters

The effective quark masses and coupling parameters were extracted from the conventional hadron masses [82]. One can find details about the extraction procedure in [74,76,78]. The quark masses that we obtained were $m_c = 1724.1$ MeV, $m_b = 5054.4$ MeV, $m_n = 361.8$ MeV, and $m_s = 542.4$ MeV. The coupling parameters are listed in Table 1. Note that the quark masses were adopted only when the upper limits for the tetraquark masses with Equation (2) were estimated.

Table 1. Effective coupling parameters C_{ij} in MeV units.

C_{ij}	c	b	$C_{i\bar{j}}$	$\bar{c}$	$\bar{b}$
n	4.0	1.3	n	6.6	2.1
s	4.3	1.3	s	6.7	2.3
c	3.2	2.0	c	5.3	3.3
b		1.9	b		2.9

Our results from Equation (4) rely on the effective quark mass gaps Δ_{cs}, Δ_{sn}, Δ_{bs}, Δ_{bc}, and Δ_{cn}, which can also be extracted from the conventional hadron masses. The values $\Delta_{bc} = 3340.2$ MeV, $\Delta_{cn} = 1280.7$ MeV, and $\Delta_{sn} = 90.6$ MeV were fixed in [73,74]. Table 2 shows the extracted Δ_{cs} and Δ_{bs} by using various hadrons. We adopted $\Delta_{cs} = 1180.6$ MeV and $\Delta_{bs} = 4520.2$ MeV in our calculations. The $X(4140)$ mass was taken to be 4146.5 MeV [82]. The corresponding CMI eigenvalue was -85.5 MeV, and then we obtained $\tilde{m} = 4232.0$ MeV. To estimate the lower limits for the tetraquark masses with Equation (3) and calculate the decay widths, we also needed the following meson masses: $M(D) = 1867.2$ MeV, $M(D^*) = 2008.6$ MeV, $M(D_s) = 1968.3$ MeV, $M(D_s^*) = 2112.2$ MeV, $M(\eta_c) = 2983.9$ MeV, $M(J/\psi) = 3096.9$ MeV, $M(B) = 5279.5$ MeV, $M(B^*) = 5324.7$ MeV, $M(B_s) = 5366.9$ MeV, $M(B_s^*) = 5415.4$ MeV, $M(\eta_b) = 9399.0$ MeV, $m(\Upsilon) = 9460.3$ MeV, $M(B_c) = 6274.9$ MeV, and $M(B_c^*) = 6344.9$ MeV. Note that the mass of the undiscovered B_c^* was calculated within the CMI model.

Even though we employed an oversimplified scheme to study the rearrangement decays, we still encountered the problem of determining the value of constant $\mathcal{C}$ because it may be different from system to system, and its determined value depends on the considered decay channels. For the $cs\bar{c}\bar{s}$ system, $\mathcal{C}$ is around 7.3 GeV [75] when the assumption that the total decay width of $X(4140)$ is equal to the sum of the partial widths of the rearrangement decay channels is used. For the $cc\bar{c}\bar{c}$ case, $\mathcal{C}$ is around 15 GeV if $X(6600)$ is treated as the ground scalar tetraquark and $M = 6552$ MeV and $\Gamma_{total} = 124$ MeV [83] values are used, along with a similar decay assumption. At present, since no triply

heavy tetraquark candidate has been observed, we just present the width results with $\mathcal{C} = 14,954.7$ MeV.

Table 2. Quark mass gaps Δ_{cs} and Δ_{bs} (units: MeV) determined from various conventional hadron masses.

Hadron	Hadron	Δ_{cs}	Hadron	Hadron	Δ_{bs}
J/ψ	ϕ	1049.4	Υ	ϕ	4237.5
$J/\psi(\eta_c)$	$D_s^*(D_s)$	992.2 (993.2)	$\Upsilon(\eta_b)$	$B_s^*(B_s)$	4041.7 (4041.8)
$D^*(D)$	$K^*(K)$	1180.6 (1179.4)	$B^*(B)$	$K^*(K)$	4520.2 (4518.8)
D_s	ϕ	1106.6	B_s	ϕ	4433.8
B_c	B_s	924.1	B_c	D_s	4252.2
Λ_c	Λ	1170.8	Λ_b	Λ	4503.8
$\Sigma_c^*(\Sigma_c)$	$\Sigma^*(\Sigma)$	1176.2 (1178.4)	$\Sigma_b^*(\Sigma_b)$	$\Sigma^*(\Sigma)$	4506.1 (4509.5)
$\Xi_c^*(\Xi_c')$	$\Xi^*(\Xi)$	1137.3 (1159.1)	$\Xi_b^*(\Xi_b')$	$\Xi^*(\Xi)$	4463.2 (4483.7)
Ω_c^*	Ω	1100.3	Ω_b	Ω	4415.5
Ξ_{cc}	Ξ	1112.2			

With the above determined parameters, the numerical results for the mass spectra and rearrangement decay widths of the triply heavy tetraquarks $cc\bar{Q}\bar{q}$, $bb\bar{Q}\bar{q}$, and $bc\bar{Q}\bar{q}$ could be calculated. We display the relative positions for all the considered states in Figure 1. Details about their masses and widths are listed in Tables 3–8.

Table 3. Numerical results for the $cc\bar{Q}\bar{q}$ systems in MeV units. The lower limits for the tetraquark masses in the seventh column were calculated using the reference meson–meson states $J/\psi D$, $J/\psi D_s$, $B_c D$, and $B_c D_s$ for the $cc\bar{c}\bar{n}$, $cc\bar{c}\bar{s}$, $cc\bar{b}\bar{n}$, and $cc\bar{b}\bar{s}$ systems, respectively. The tetraquark masses in the sixth column were calculated by using $X(4140)$ as the reference state. The corresponding $\langle H_{CMI}\rangle$ base vectors are given in Section 2.2.

System	J^P	$\langle H_{CMI}\rangle$	Eigenvalue	Eigenvector	Mass	Lower Limit	Upper Limit
$cc\bar{c}\bar{n}$	2^+	(50.9)	(50.9)	$[\{1.00\}]$	(5372.0)	(5092.4)	(5585.0)
	1^+	$\begin{pmatrix} -12.5 & -4.9 & -10.4 \\ -4.9 & -23.5 & -67.3 \\ -10.4 & -67.3 & 7.5 \end{pmatrix}$	$\begin{pmatrix} 61.4 \\ -11.3 \\ -78.7 \end{pmatrix}$	$\begin{bmatrix} \{-0.07,-0.62,0.78\} \\ \{0.99,-0.16,-0.04\} \\ \{-0.15,-0.77,-0.62\} \end{bmatrix}$	$\begin{pmatrix} 5382.5 \\ 5309.8 \\ 5242.4 \end{pmatrix}$	$\begin{pmatrix} 5102.9 \\ 5030.2 \\ 4962.8 \end{pmatrix}$	$\begin{pmatrix} 5595.5 \\ 5522.8 \\ 5455.4 \end{pmatrix}$
	0^+	$\begin{pmatrix} -44.3 & 116.6 \\ 116.6 & 28.8 \end{pmatrix}$	$\begin{pmatrix} 114.5 \\ -129.9 \end{pmatrix}$	$\begin{bmatrix} \{-0.59,-0.81\} \\ \{-0.81,0.59\} \end{bmatrix}$	$\begin{pmatrix} 5435.5 \\ 5191.1 \end{pmatrix}$	$\begin{pmatrix} 5155.9 \\ 4911.5 \end{pmatrix}$	$\begin{pmatrix} 5648.6 \\ 5404.2 \end{pmatrix}$
$cc\bar{c}\bar{s}$	2^+	(52.0)	(52.0)	$[\{1.00\}]$	(5463.7)	(5196.1)	(5766.7)
	1^+	$\begin{pmatrix} -12.0 & -5.3 & -11.2 \\ -5.3 & -25.9 & -67.9 \\ -11.2 & -67.9 & 7.1 \end{pmatrix}$	$\begin{pmatrix} 60.9 \\ -10.6 \\ -81.0 \end{pmatrix}$	$\begin{bmatrix} \{-0.08,-0.61,0.79\} \\ \{0.98,-0.17,-0.04\} \\ \{-0.16,-0.77,-0.62\} \end{bmatrix}$	$\begin{pmatrix} 5472.5 \\ 5401.0 \\ 5330.6 \end{pmatrix}$	$\begin{pmatrix} 5205.0 \\ 5133.5 \\ 5063.1 \end{pmatrix}$	$\begin{pmatrix} 5775.6 \\ 5704.1 \\ 5633.7 \end{pmatrix}$
	0^+	$\begin{pmatrix} -44.0 & 117.6 \\ 117.6 & 30.0 \end{pmatrix}$	$\begin{pmatrix} 116.3 \\ -130.3 \end{pmatrix}$	$\begin{bmatrix} \{-0.59,-0.81\} \\ \{-0.81,0.59\} \end{bmatrix}$	$\begin{pmatrix} 5527.9 \\ 5281.4 \end{pmatrix}$	$\begin{pmatrix} 5260.4 \\ 5013.9 \end{pmatrix}$	$\begin{pmatrix} 5831.0 \\ 5584.4 \end{pmatrix}$
$cc\bar{b}\bar{n}$	2^+	(38.4)	(38.4)	$[\{1.00\}]$	(8699.1)	(8338.9)	(8902.8)
	1^+	$\begin{pmatrix} -14.4 & -12.4 & -26.4 \\ -12.4 & -1.9 & -56.0 \\ -26.4 & -56.0 & 11.1 \end{pmatrix}$	$\begin{pmatrix} 62.8 \\ -2.0 \\ -66.0 \end{pmatrix}$	$\begin{bmatrix} \{-0.16,-0.63,0.76\} \\ \{0.87,-0.45,-0.19\} \\ \{-0.47,-0.63,-0.62\} \end{bmatrix}$	$\begin{pmatrix} 8723.5 \\ 8658.7 \\ 8594.6 \end{pmatrix}$	$\begin{pmatrix} 8363.3 \\ 8298.5 \\ 8234.5 \end{pmatrix}$	$\begin{pmatrix} 8927.2 \\ 8862.4 \\ 8798.4 \end{pmatrix}$
	0^+	$\begin{pmatrix} -40.8 & 97.0 \\ 97.0 & 18.0 \end{pmatrix}$	$\begin{pmatrix} 90.0 \\ -112.8 \end{pmatrix}$	$\begin{bmatrix} \{-0.60,-0.80\} \\ \{-0.80,0.60\} \end{bmatrix}$	$\begin{pmatrix} 8750.6 \\ 8547.9 \end{pmatrix}$	$\begin{pmatrix} 8390.5 \\ 8187.7 \end{pmatrix}$	$\begin{pmatrix} 8954.4 \\ 8751.6 \end{pmatrix}$
$cc\bar{b}\bar{s}$	2^+	(38.7)	(38.7)	$[\{1.00\}]$	(8789.9)	(8441.9)	(9083.7)
	1^+	$\begin{pmatrix} -14.7 & -12.8 & -27.2 \\ -12.8 & -1.9 & -56.6 \\ -27.2 & -56.6 & 11.1 \end{pmatrix}$	$\begin{pmatrix} 63.5 \\ -1.7 \\ -67.2 \end{pmatrix}$	$\begin{bmatrix} \{-0.16,-0.63,0.76\} \\ \{0.87,-0.46,-0.20\} \\ \{-0.47,-0.63,-0.62\} \end{bmatrix}$	$\begin{pmatrix} 8814.7 \\ 8749.5 \\ 8684.0 \end{pmatrix}$	$\begin{pmatrix} 8466.7 \\ 8401.5 \\ 8336.0 \end{pmatrix}$	$\begin{pmatrix} 9108.5 \\ 9043.3 \\ 8977.8 \end{pmatrix}$
	0^+	$\begin{pmatrix} -41.3 & 98.0 \\ 98.0 & 18.0 \end{pmatrix}$	$\begin{pmatrix} 90.7 \\ -114.0 \end{pmatrix}$	$\begin{bmatrix} \{-0.60,-0.80\} \\ \{-0.80,0.60\} \end{bmatrix}$	$\begin{pmatrix} 8842.0 \\ 8637.2 \end{pmatrix}$	$\begin{pmatrix} 8493.9 \\ 8289.2 \end{pmatrix}$	$\begin{pmatrix} 9135.7 \\ 8931.0 \end{pmatrix}$

Table 4. Rearrangement decays for the $cc\bar{c}\bar{n}$, $cc\bar{c}\bar{s}$, $cc\bar{b}\bar{n}$, and $cc\bar{b}\bar{s}$ states. The numbers in the parentheses are $(100|\mathcal{M}|^2/\mathcal{C}^2, \Gamma)$. The tetraquark mass, partial width Γ, and total width Γ_{sum} values are given in MeV units.

System	J^P	Mass	Decay Channels			Γ_{sum}
$cc\bar{c}\bar{n}$			$J/\psi D^*$			
	2^+	[5372.0]	[(33.3, 168.2)]			[168.2]
			$J/\psi D^*$	$J/\psi D$	$\eta_c D^*$	
	1^+	[5382.5 5309.8 5242.4]	[(49.6, 254.5) (0.2, 0.8) (0.2, 0.7)]	[(1.3, 8.0) (11.4, 66.0) (29.0, 153.6)]	[(2.9, 17.6) (21.8, 122.3) (17.0, 86.4)]	[280.0 189.1 240.8]
			$J/\psi D^*$	$\eta_c D$		
	0^+	[5435.5 5191.1]	[(54.9, 302.0) (3.5, 10.5)]	[(0.1, 0.8) (41.6, 247.6)]		[302.8 258.1]
$cc\bar{c}\bar{s}$			$J/\psi D_s^*$			
	2^+	[5463.7]	[(33.3, 161.1)]			[161.1]
			$J/\psi D_s^*$	$J/\psi D_s$	$\eta_c D_s^*$	
	1^+	[5472.5 5401.0 5330.6]	[(49.6, 243.2) (0.2, 1.0) (0.2, 0.6)]	[(1.3, 7.8) (11.3, 63.4) (29.0, 147.6)]	[(3.1, 18.2) (21.8, 117.5) (16.7, 80.9)]	[269.2 181.9 229.1]
			$J/\psi D_s^*$	$\eta_c D_s$		
	0^+	[5527.9 5281.4]	[(54.9, 291.0) (3.4, 9.4)]	[(0.1, 0.8) (41.6, 238.8)]		[291.8 248.2]
$cc\bar{b}\bar{n}$			$B_c^* D^*$			
	2^+	[8699.1]	[(33.3, 82.5)]			[82.5]
			$B_c^* D^*$	$B_c^* D$	$B_c D^*$	
	1^+	[8723.5 8658.7 8594.6]	[(48.5, 123.6) (0.5, 1.3) (1.0, 2.1)]	[(0.4, 1.2) (2.1, 5.8) (39.2, 102.1)]	[(3.8, 10.5) (32.0, 83.2) (5.9, 14.2)]	[135.4 90.3 118.4]
			$B_c^* D^*$	$B_c D$		
	0^+	[8750.6 8547.9]	[(54.7, 144.0) (3.6, 6.8)]	[(0.1, 0.3) (41.6, 112.9)]		[144.3 119.7]
$cc\bar{b}\bar{s}$			$B_c^* D_s^*$			
	2^+	[8789.9]	[(33.3, 80.6)]			[80.6]
			$B_c^* D_s^*$	$B_c^* D_s$	$B_c D_s^*$	
	1^+	[8814.7 8749.5 8684.0]	[(48.4, 120.9) (0.6, 1.3) (1.0, 2.1)]	[(0.4, 1.2) (2.0, 5.5) (39.3, 100.5)]	[(3.8, 10.5) (32.0, 81.7) (5.8, 13.5)]	[132.6 88.4 116.0]
			$B_c^* D^*$	$B_c D$		
	0^+	[8842.0 8637.2]	[(54.7, 141.1) (3.6, 6.6)]	[(0.1, 0.3) (41.6, 110.9)]		[141.4 117.4]

Table 5. Numerical results for the $bb\bar{Q}\bar{q}$ systems in MeV units. The lower limits for the tetraquark masses in the seventh column were calculated using the reference meson–meson states $B_c^- \bar{B}$, $B_c^- \bar{B}_s^0$, $\Upsilon\bar{B}$, and $\Upsilon\bar{B}_s^0$ for the $bb\bar{c}\bar{n}$, $bb\bar{c}\bar{s}$, $bb\bar{b}\bar{n}$, and $bb\bar{b}\bar{s}$ systems, respectively. The tetraquark masses in the sixth column were calculated using $X(4140)$ as the reference state. The corresponding $\langle H_{CMI} \rangle$ base vectors are given in Section 2.2.

System	J^P	$\langle H_{CMI} \rangle$	Eigenvalue	Eigenvector	Mass	Lower Limit	Upper Limit
$bb\bar{c}\bar{n}$	2^+	(30.1)	(30.1)	[{1.00}]	(12,020.9)	(11,670.9)	(12,224.8)
	1^+	(1.3 4.5 9.6 4.5 −26.9 −30.5 9.6 −30.5 2.3)	(23.1 1.4 −47.8)	[{0.27, −0.48, 0.83} {0.95, 0.29, −0.13} {0.18, −0.82, −0.54}]	(12,013.9 11,992.2 11,942.9)	(11,663.9 11,642.2 11,593.0)	(12,217.8 12,196.1 12,146.9)
	0^+	(−13.1 52.9 52.9 23.6)	(61.3 −50.7)	[{0.58, 0.81} {−0.81, 0.58}]	(12,052.0 11,940.0)	(11,702.1 11,590.1)	(12,256.0 12,144.0)

Table 5. *Cont.*

System	J^P	$\langle H_{CMI} \rangle$	Eigenvalue	Eigenvector	Mass	Lower Limit	Upper Limit
$bb\bar{c}\bar{s}$	2^+	(31.5)	(31.5)	$[\{1.00\}]$	$(12{,}122.9)$	$(11{,}762.9)$	$(12{,}406.8)$
	1^+	$\begin{pmatrix} 1.6 & 3.8 & 8.0 \\ 3.8 & -29.3 & -31.7 \\ 8.0 & -31.7 & 1.9 \end{pmatrix}$	$\begin{pmatrix} 22.7 \\ 1.5 \\ -50.1 \end{pmatrix}$	$\begin{bmatrix} \{0.23, -0.49, 0.84\} \\ \{0.96, 0.24, -0.12\} \\ \{0.14, -0.84, -0.53\} \end{bmatrix}$	$\begin{pmatrix} 12{,}114.2 \\ 12{,}093.0 \\ 12{,}041.3 \end{pmatrix}$	$\begin{pmatrix} 11{,}754.1 \\ 11{,}732.9 \\ 11{,}681.3 \end{pmatrix}$	$\begin{pmatrix} 12{,}398.0 \\ 12{,}376.8 \\ 12{,}325.2 \end{pmatrix}$
	0^+	$\begin{pmatrix} -13.3 & 54.9 \\ 54.9 & 24.8 \end{pmatrix}$	$\begin{pmatrix} 63.8 \\ -52.4 \end{pmatrix}$	$\begin{bmatrix} \{0.58, 0.81\} \\ \{-0.81, 0.58\} \end{bmatrix}$	$\begin{pmatrix} 12{,}155.3 \\ 12{,}039.1 \end{pmatrix}$	$\begin{pmatrix} 11{,}795.2 \\ 11{,}679.1 \end{pmatrix}$	$\begin{pmatrix} 12{,}439.1 \\ 12{,}322.9 \end{pmatrix}$
$bb\bar{b}\bar{n}$	2^+	(21.9)	(21.9)	$[\{1.00\}]$	$(15{,}352.8)$	$(14{,}779.8)$	$(15{,}546.9)$
	1^+	$\begin{pmatrix} -4.8 & 3.0 & 6.4 \\ 3.0 & -5.3 & -28.3 \\ 6.4 & -28.3 & 5.9 \end{pmatrix}$	$\begin{pmatrix} 29.4 \\ -3.5 \\ -30.2 \end{pmatrix}$	$\begin{bmatrix} \{0.09, -0.62, 0.78\} \\ \{0.97, 0.25, 0.09\} \\ \{0.25, -0.74, -0.62\} \end{bmatrix}$	$\begin{pmatrix} 15{,}360.3 \\ 15{,}327.5 \\ 15{,}300.8 \end{pmatrix}$	$\begin{pmatrix} 14{,}787.3 \\ 14{,}754.5 \\ 14{,}727.8 \end{pmatrix}$	$\begin{pmatrix} 15{,}554.4 \\ 15{,}521.5 \\ 15{,}494.8 \end{pmatrix}$
	0^+	$\begin{pmatrix} -18.1 & 49.0 \\ 49.0 & 12.8 \end{pmatrix}$	$\begin{pmatrix} 48.7 \\ -54.0 \end{pmatrix}$	$\begin{bmatrix} \{-0.59, -0.81\} \\ \{-0.81, 0.59\} \end{bmatrix}$	$\begin{pmatrix} 15{,}379.7 \\ 15{,}276.9 \end{pmatrix}$	$\begin{pmatrix} 14{,}806.6 \\ 14{,}703.9 \end{pmatrix}$	$\begin{pmatrix} 15{,}573.7 \\ 15{,}471.0 \end{pmatrix}$
$bb\bar{b}\bar{s}$	2^+	(22.4)	(22.4)	$[\{1.00\}]$	$(15{,}454.1)$	$(14{,}870.9)$	$(15{,}728.0)$
	1^+	$\begin{pmatrix} -5.3 & 2.3 & 4.8 \\ 2.3 & -5.3 & -29.4 \\ 4.8 & -29.4 & 5.9 \end{pmatrix}$	$\begin{pmatrix} 30.4 \\ -4.6 \\ -30.6 \end{pmatrix}$	$\begin{bmatrix} \{0.06, -0.63, 0.77\} \\ \{0.98, 0.18, 0.07\} \\ \{0.19, -0.75, -0.63\} \end{bmatrix}$	$\begin{pmatrix} 15{,}462.0 \\ 15{,}427.1 \\ 15{,}401.1 \end{pmatrix}$	$\begin{pmatrix} 14{,}878.9 \\ 14{,}844.0 \\ 14{,}817.9 \end{pmatrix}$	$\begin{pmatrix} 15{,}736.0 \\ 15{,}701.0 \\ 15{,}675.0 \end{pmatrix}$
	0^+	$\begin{pmatrix} -19.2 & 50.9 \\ 50.9 & 12.8 \end{pmatrix}$	$\begin{pmatrix} 50.2 \\ -56.6 \end{pmatrix}$	$\begin{bmatrix} \{-0.59, -0.81\} \\ \{-0.81, 0.59\} \end{bmatrix}$	$\begin{pmatrix} 15{,}481.9 \\ 15{,}375.1 \end{pmatrix}$	$\begin{pmatrix} 14{,}898.7 \\ 14{,}791.9 \end{pmatrix}$	$\begin{pmatrix} 15{,}755.8 \\ 15{,}649.0 \end{pmatrix}$

Table 6. Rearrangement decays for the $bb\bar{c}\bar{n}$, $bb\bar{c}\bar{s}$, $bb\bar{b}\bar{n}$, and $bb\bar{b}\bar{s}$ states. The numbers in the parentheses are $(100|\mathcal{M}|^2/\mathcal{C}^2, \Gamma)$. The tetraquark mass, partial width Γ, and total width Γ_{sum} values are given in MeV units.

System	J^P	Mass	Decay Channels			Γ_{sum}
$bb\bar{c}\bar{n}$			$B_c^{*-}\bar{B}^*$			
	2^+	$[12{,}020.9]$	$[(33.3, 59.0)]$			$[59.0]$
			$B_c^{*-}\bar{B}^*$	$B_c^{*-}\bar{B}$	$B_c^{-}\bar{B}^*$	
	1^+	$\begin{bmatrix} 12{,}013.9 \\ 11{,}992.2 \\ 11{,}942.9 \end{bmatrix}$	$\begin{bmatrix} (46.1, 80.8) \\ (3.9, 6.6) \\ (0.1, 0.1) \end{bmatrix}$	$\begin{bmatrix} (9.6, 17.8) \\ (17.4, 31.6) \\ (14.7, 25.0) \end{bmatrix}$	$\begin{bmatrix} (0.8, 1.6) \\ (12.6, 23.7) \\ (28.2, 49.8) \end{bmatrix}$	$\begin{bmatrix} 100.2 \\ 61.9 \\ 75.0 \end{bmatrix}$
			$B_c^{*-}\bar{B}^*$	$B_c^{-}\bar{B}$		
	0^+	$\begin{bmatrix} 12{,}052.0 \\ 11{,}940.0 \end{bmatrix}$	$\begin{bmatrix} (55.3, 101.6) \\ (3.1, 4.8) \end{bmatrix}$	$\begin{bmatrix} (0.2, 0.4) \\ (41.5, 77.7) \end{bmatrix}$		$\begin{bmatrix} 102.0 \\ 82.5 \end{bmatrix}$
$bb\bar{c}\bar{s}$			$B_c^{*-}\bar{B}_s^{*0}$			
	2^+	$[12{,}122.9]$	$[(33.3, 59.2)]$			$[59.2]$
			$B_c^{*-}\bar{B}_s^{*0}$	$B_c^{*-}\bar{B}_s^{0}$	$B_c^{-}\bar{B}_s^{*0}$	
	1^+	$\begin{bmatrix} 12{,}114.2 \\ 12{,}093.0 \\ 12{,}041.3 \end{bmatrix}$	$\begin{bmatrix} (47.0, 82.7) \\ (2.8, 4.9) \\ (0.1, 0.2) \end{bmatrix}$	$\begin{bmatrix} (8.6, 16.1) \\ (17.1, 31.2) \\ (16.0, 27.3) \end{bmatrix}$	$\begin{bmatrix} (1.1, 2.2) \\ (13.9, 26.1) \\ (26.7, 47.1) \end{bmatrix}$	$\begin{bmatrix} 100.9 \\ 62.2 \\ 74.6 \end{bmatrix}$
			$B_c^{*-}\bar{B}_s^{*0}$	$B_c\bar{B}_s^{0}$		
	0^+	$\begin{bmatrix} 12{,}155.3 \\ 12{,}039.1 \end{bmatrix}$	$\begin{bmatrix} (55.3, 102.0) \\ (3.0, 4.8) \end{bmatrix}$	$\begin{bmatrix} (0.2, 0.4) \\ (41.5, 77.9) \end{bmatrix}$		$\begin{bmatrix} 102.4 \\ 82.7 \end{bmatrix}$
$bb\bar{b}\bar{n}$			$\Upsilon\bar{B}^*$			
	2^+	$[15{,}352.8]$	$[(33.3, 50.1)]$			$[50.1]$
			$\Upsilon\bar{B}^*$	$\Upsilon\bar{B}$	$\eta_b\bar{B}^*$	
	1^+	$\begin{bmatrix} 15{,}360.3 \\ 15{,}327.5 \\ 15{,}300.8 \end{bmatrix}$	$\begin{bmatrix} (49.4, 74.7) \\ (0.3, 0.4) \\ (0.3, 0.5) \end{bmatrix}$	$\begin{bmatrix} (3.0, 4.7) \\ (25.1, 38.4) \\ (13.6, 20.4) \end{bmatrix}$	$\begin{bmatrix} (1.0, 1.6) \\ (8.3, 12.8) \\ (32.4, 49.4) \end{bmatrix}$	$\begin{bmatrix} 81.0 \\ 51.6 \\ 70.3 \end{bmatrix}$
			$\Upsilon\bar{B}^*$	$\eta_b\bar{B}$		
	0^+	$\begin{bmatrix} 15{,}379.7 \\ 15{,}276.9 \end{bmatrix}$	$\begin{bmatrix} (54.9, 84.3) \\ (3.4, 4.8) \end{bmatrix}$	$\begin{bmatrix} (0.1, 0.2) \\ (41.6, 64.6) \end{bmatrix}$		$\begin{bmatrix} 84.5 \\ 69.4 \end{bmatrix}$
$bb\bar{b}\bar{s}$			$\Upsilon\bar{B}_s^{*0}$			
	2^+	$[15{,}454.1]$	$[(33.3, 50.2)]$			$[50.2]$
			$\Upsilon\bar{B}_s^{*0}$	$\Upsilon\bar{B}_s^{0}$	$\eta_b\bar{B}_s^{*0}$	
	1^+	$\begin{bmatrix} 15{,}462.0 \\ 15{,}427.1 \\ 15{,}401.1 \end{bmatrix}$	$\begin{bmatrix} (49.5, 75.1) \\ (0.1, 0.2) \\ (0.3, 0.5) \end{bmatrix}$	$\begin{bmatrix} (2.5, 4.0) \\ (23.3, 35.7) \\ (15.9, 23.9) \end{bmatrix}$	$\begin{bmatrix} (1.1, 1.8) \\ (10.1, 15.7) \\ (30.4, 46.4) \end{bmatrix}$	$\begin{bmatrix} 80.8 \\ 51.6 \\ 70.8 \end{bmatrix}$
			$\Upsilon\bar{B}_s^{*0}$	$\eta_b\bar{B}_s^{0}$		
	0^+	$\begin{bmatrix} 15{,}481.9 \\ 15{,}375.1 \end{bmatrix}$	$\begin{bmatrix} (54.9, 84.4) \\ (3.5, 4.9) \end{bmatrix}$	$\begin{bmatrix} (0.1, 0.2) \\ (41.6, 64.7) \end{bmatrix}$		$\begin{bmatrix} 84.6 \\ 69.6 \end{bmatrix}$

Table 7. Numerical results for the $bc\bar{Q}\bar{q}$ systems in MeV units. The tetraquark mass lower limits in the seventh column were calculated using the reference meson–meson states $B_c^- D$, $B_c^- D_s^+$, ΥD, and ΥD_s^+ for the $bc\bar{c}\bar{n}$, $bc\bar{c}\bar{s}$, $bc\bar{b}\bar{n}$, and $bc\bar{b}\bar{s}$ systems, respectively. The tetraquark masses in the sixth column were calculated using $X(4140)$ as the reference state. The corresponding $\langle H_{CMI}\rangle$ base vectors are given in Section 2.2.

System	J^P	$\langle H_{CMI}\rangle$	Eigenvalue	Eigenvector	Mass	Lower Limit	Upper Limit
$bc\bar{c}\bar{n}$	2^+	$\begin{pmatrix} 49.7 & -7.1 \\ -7.1 & 39.1 \end{pmatrix}$	$\begin{pmatrix} 53.2 \\ 35.5 \end{pmatrix}$	$\begin{bmatrix} \{-0.89, 0.45\} \\ \{-0.45, -0.89\} \end{bmatrix}$	$\begin{pmatrix} 8713.9 \\ 8696.2 \end{pmatrix}$	$\begin{pmatrix} 8353.7 \\ 8336.0 \end{pmatrix}$	$\begin{pmatrix} 8917.6 \\ 8899.9 \end{pmatrix}$
	1^+	$\begin{pmatrix} -65.7 & -0.47 & 30.64 & 7.07 & 26.00 & -0.40 \\ -0.47 & 13.33 & 8.33 & 26.00 & 0.00 & -48.93 \\ 30.64 & 8.33 & 2.67 & -0.40 & -48.93 & 0.00 \\ 7.07 & 26.00 & -0.40 & -7.07 & -0.19 & 12.26 \\ 26.00 & 0.00 & -48.93 & -0.19 & -26.67 & 3.33 \\ -0.40 & -48.93 & 0.00 & 12.26 & 3.33 & -5.33 \end{pmatrix}$	$\begin{pmatrix} 58.8 \\ 37.8 \\ 4.6 \\ -26.7 \\ -58.4 \\ -104.8 \end{pmatrix}$	$\begin{bmatrix} \{0.04, 0.75, 0.28, 0.20, -0.17, -0.54\} \\ \{0.09, -0.24, 0.77, -0.07, -0.54, 0.21\} \\ \{0.14, 0.12, 0.04, 0.85, 0.10, 0.48\} \\ \{0.67, -0.03, 0.35, -0.16, 0.63, -0.05\} \\ \{-0.12, 0.60, 0.03, -0.44, 0.07, 0.65\} \\ \{0.71, 0.08, -0.45, -0.09, -0.52, 0.07\} \end{bmatrix}$	$\begin{pmatrix} 8719.4 \\ 8698.4 \\ 8665.3 \\ 8633.9 \\ 8602.3 \\ 8555.9 \end{pmatrix}$	$\begin{pmatrix} 8359.3 \\ 8338.3 \\ 8305.2 \\ 8273.8 \\ 8242.1 \\ 8195.7 \end{pmatrix}$	$\begin{pmatrix} 8923.2 \\ 8902.2 \\ 8869.0 \\ 8837.7 \\ 8806.0 \\ 8759.6 \end{pmatrix}$
	0^+	$\begin{pmatrix} -30.13 & -5.77 & 14.14 & 84.75 \\ -5.77 & -48.00 & 84.75 & 0.00 \\ 14.14 & 84.75 & -123.33 & -14.43 \\ 84.75 & 0.00 & -14.43 & 24.0 \end{pmatrix}$	$\begin{pmatrix} 86.2 \\ 7.3 \\ -88.4 \\ -182.5 \end{pmatrix}$	$\begin{bmatrix} \{0.59, -0.05, -0.04, 0.81\} \\ \{0.09, 0.83, 0.55, 0.01\} \\ \{0.79, -0.17, 0.14, -0.58\} \\ \{-0.17, -0.53, 0.82, 0.13\} \end{bmatrix}$	$\begin{pmatrix} 8746.8 \\ 8668.0 \\ 8572.2 \\ 8478.1 \end{pmatrix}$	$\begin{pmatrix} 8386.7 \\ 8307.8 \\ 8212.1 \\ 8118.0 \end{pmatrix}$	$\begin{pmatrix} 8950.6 \\ 8871.7 \\ 8776.0 \\ 8681.9 \end{pmatrix}$
$bc\bar{c}\bar{s}$	2^+	$\begin{pmatrix} 50.27 & -6.79 \\ -6.79 & 40.27 \end{pmatrix}$	$\begin{pmatrix} 53.7 \\ 36.8 \end{pmatrix}$	$\begin{bmatrix} \{-0.89, 0.45\} \\ \{-0.45, -0.89\} \end{bmatrix}$	$\begin{pmatrix} 8805.0 \\ 8788.1 \end{pmatrix}$	$\begin{pmatrix} 8456.9 \\ 8440.0 \end{pmatrix}$	$\begin{pmatrix} 9098.7 \\ 9081.8 \end{pmatrix}$
	1^+	$\begin{pmatrix} -67.07 & -1.89 & 30.17 & 6.79 & 25.60 & -1.60 \\ -1.89 & 14.53 & 8.00 & 25.60 & 0.00 & -49.78 \\ 30.17 & 8.00 & 2.27 & -1.60 & -49.78 & 0.00 \\ 6.79 & 25.60 & -1.60 & -6.67 & -0.75 & 12.07 \\ 25.60 & 0.00 & -49.78 & -0.75 & 29.07 & 3.20 \\ -1.60 & -49.78 & 0.00 & 12.07 & 3.20 & -4.53 \end{pmatrix}$	$\begin{pmatrix} 60.0 \\ 37.9 \\ 4.3 \\ -28.9 \\ -57.5 \\ -106.4 \end{pmatrix}$	$\begin{bmatrix} \{0.03, 0.76, 0.25, 0.19, -0.15, -0.56\} \\ \{0.09, -0.21, 0.79, -0.08, -0.54, 0.18\} \\ \{0.10, 0.13, 0.03, 0.86, 0.05, 0.47\} \\ \{0.68, -0.03, 0.35, -0.10, 0.63, -0.05\} \\ \{-0.11, 0.60, 0.05, -0.44, 0.10, 0.65\} \\ \{0.71, 0.10, -0.45, -0.09, -0.53, 0.09\} \end{bmatrix}$	$\begin{pmatrix} 8811.3 \\ 8789.2 \\ 8755.6 \\ 8722.4 \\ 8693.8 \\ 8644.8 \end{pmatrix}$	$\begin{pmatrix} 8463.2 \\ 8441.1 \\ 8407.6 \\ 8374.3 \\ 8345.7 \\ 8296.8 \end{pmatrix}$	$\begin{pmatrix} 9105.0 \\ 9082.9 \\ 9049.3 \\ 9016.1 \\ 8987.5 \\ 8938.6 \end{pmatrix}$
	0^+	$\begin{pmatrix} -30.13 & -5.54 & 13.58 & 86.22 \\ -5.54 & -50.40 & 86.22 & 0.00 \\ 13.58 & 86.22 & -125.73 & 13.86 \\ 86.22 & 0.00 & -13.86 & 25.20 \end{pmatrix}$	$\begin{pmatrix} 88.3 \\ 6.2 \\ -89.8 \\ -185.8 \end{pmatrix}$	$\begin{bmatrix} \{0.59, -0.04, -0.03, 0.81\} \\ \{0.09, 0.83, 0.55, 0.00\} \\ \{0.79, -0.16, 0.13, -0.58\} \\ \{-0.16, -0.53, 0.82, 0.12\} \end{bmatrix}$	$\begin{pmatrix} 8839.6 \\ 8757.5 \\ 8661.5 \\ 8565.4 \end{pmatrix}$	$\begin{pmatrix} 8491.5 \\ 8409.5 \\ 8313.4 \\ 8217.4 \end{pmatrix}$	$\begin{pmatrix} 9133.3 \\ 9051.2 \\ 8955.2 \\ 8859.2 \end{pmatrix}$

Table 7. *Cont.*

System	J^P	$\langle H_{CMI} \rangle$	Eigenvalue	Eigenvector	Mass	Lower Limit	Upper Limit
$bc\bar{b}\bar{n}$	2^+	$\begin{pmatrix} 45.27 & -11.60 \\ -11.60 & 28.67 \end{pmatrix}$	$\begin{pmatrix} 51.2 \\ 22.7 \end{pmatrix}$	$\begin{bmatrix} \{-0.89, 0.46\} \\ \{-0.46, -0.89\} \end{bmatrix}$	$\begin{pmatrix} 12{,}042.0 \\ 12{,}013.5 \end{pmatrix}$	$\begin{pmatrix} 11{,}468.9 \\ 11{,}440.4 \end{pmatrix}$	$\begin{pmatrix} 12{,}245.9 \\ 12{,}217.4 \end{pmatrix}$
	1^+	$\begin{pmatrix} -54.07 & -11.79 & 23.10 & 11.60 & 19.60 & -10.00 \\ -11.79 & 2.53 & 13.67 & 19.60 & 0.00 & -42.14 \\ 23.10 & 13.67 & 6.27 & -10.00 & -42.14 & 0.00 \\ 11.60 & 19.60 & -10.00 & -11.07 & -4.71 & 9.24 \\ 19.60 & 0.00 & -42.14 & -4.71 & -5.07 & 5.47 \\ -10.00 & -42.14 & 0.00 & 9.24 & 5.47 & -12.53 \end{pmatrix}$	$\begin{pmatrix} 51.4 \\ 32.3 \\ -3.5 \\ -17.5 \\ -43.3 \\ -93.3 \end{pmatrix}$	$\begin{bmatrix} \{0.03, 0.50, 0.61, 0.05, -0.49, -0.37\} \\ \{-0.03, 0.60, -0.46, 0.23, 0.41, -0.46\} \\ \{0.02, 0.08, -0.03, 0.89, -0.18, 0.41\} \\ \{0.66, -0.06, 0.46, 0.12, 0.58, 0.00\} \\ \{-0.35, 0.52, 0.23, -0.25, 0.32, 0.62\} \\ \{0.67, 0.33, -0.38, -0.27, -0.36, 0.31\} \end{bmatrix}$	$\begin{pmatrix} 12{,}042.1 \\ 12{,}023.1 \\ 11{,}987.3 \\ 11{,}973.2 \\ 11{,}947.5 \\ 11{,}897.5 \end{pmatrix}$	$\begin{pmatrix} 11{,}469.0 \\ 11{,}450.0 \\ 11{,}414.2 \\ 11{,}400.1 \\ 11{,}374.3 \\ 11{,}324.4 \end{pmatrix}$	$\begin{pmatrix} 12{,}246.1 \\ 12{,}227.0 \\ 12{,}191.2 \\ 12{,}177.2 \\ 12{,}151.4 \\ 12{,}101.4 \end{pmatrix}$
	0^+	$\begin{pmatrix} -30.93 & -9.47 & 23.19 & 73.00 \\ -9.47 & -26.40 & 72.99 & 0.00 \\ 23.19 & 72.99 & -103.73 & -23.67 \\ 72.99 & 0.00 & -23.67 & 13.2 \end{pmatrix}$	$\begin{pmatrix} 68.5 \\ 17.5 \\ -72.7 \\ -161.2 \end{pmatrix}$	$\begin{bmatrix} \{0.58, -0.12, -0.08, 0.80\} \\ \{0.17, 0.83, 0.52, 0.06\} \\ \{0.73, -0.29, 0.28, -0.55\} \\ \{-0.31, -0.46, 0.80, 0.24\} \end{bmatrix}$	$\begin{pmatrix} 12{,}059.3 \\ 12{,}008.3 \\ 11{,}918.1 \\ 11{,}829.5 \end{pmatrix}$	$\begin{pmatrix} 11{,}486.2 \\ 11{,}435.2 \\ 11{,}345.0 \\ 11{,}256.4 \end{pmatrix}$	$\begin{pmatrix} 12{,}263.2 \\ 12{,}212.2 \\ 12{,}122.0 \\ 12{,}033.5 \end{pmatrix}$
$bc\bar{b}\bar{s}$	2^+	$\begin{pmatrix} 46.27 & -11.31 \\ -11.31 & 29.07 \end{pmatrix}$	$\begin{pmatrix} 51.9 \\ 23.5 \end{pmatrix}$	$\begin{bmatrix} \{-0.90, 0.44\} \\ \{-0.44, -0.90\} \end{bmatrix}$	$\begin{pmatrix} 12{,}143.3 \\ 12{,}114.9 \end{pmatrix}$	$\begin{pmatrix} 11{,}572.2 \\ 11{,}543.8 \end{pmatrix}$	$\begin{pmatrix} 12{,}427.2 \\ 12{,}398.8 \end{pmatrix}$
	1^+	$\begin{pmatrix} -55.07 & -13.20 & 22.63 & 11.31 & 19.20 & -11.20 \\ -13.20 & 2.53 & 13.33 & 19.20 & 0.00 & -42.99 \\ 22.63 & 13.33 & 6.27 & -11.20 & -42.99 & 0.00 \\ 11.31 & 19.20 & -11.20 & -11.47 & -5.28 & 9.05 \\ 19.20 & 0.00 & -42.99 & -5.28 & -5.07 & 5.33 \\ -11.20 & -42.99 & 0.00 & 9.05 & 5.33 & -12.53 \end{pmatrix}$	$\begin{pmatrix} 51.9 \\ 33.4 \\ -3.7 \\ -19.2 \\ -42.7 \\ -94.9 \end{pmatrix}$	$\begin{bmatrix} \{0.02, 0.50, 0.61, 0.03, -0.49, -0.37\} \\ \{-0.03, 0.60, -0.46, 0.22, 0.40, -0.46\} \\ \{-0.03, 0.08, -0.07, 0.88, -0.23, 0.39\} \\ \{0.67, -0.06, 0.45, 0.21, 0.55, 0.00\} \\ \{-0.33, 0.52, 0.26, -0.23, 0.34, 0.62\} \\ \{0.66, 0.34, -0.37, -0.28, -0.36, 0.32\} \end{bmatrix}$	$\begin{pmatrix} 12{,}143.3 \\ 12{,}124.9 \\ 12{,}087.7 \\ 12{,}072.2 \\ 12{,}048.7 \\ 11{,}996.6 \end{pmatrix}$	$\begin{pmatrix} 11{,}572.2 \\ 11{,}553.8 \\ 11{,}516.6 \\ 11{,}501.1 \\ 11{,}477.6 \\ 11425.4 \end{pmatrix}$	$\begin{pmatrix} 12{,}427.2 \\ 12{,}408.7 \\ 12{,}371.6 \\ 12{,}356.1 \\ 12{,}332.6 \\ 12{,}280.4 \end{pmatrix}$
	0^+	$\begin{pmatrix} -31.73 & -9.24 & 22.63 & 74.46 \\ -9.24 & -26.40 & 74.46 & 0.00 \\ 22.63 & 74.46 & -105.73 & -23.09 \\ 74.46 & 0.00 & -23.09 & 13.20 \end{pmatrix}$	$\begin{pmatrix} 69.6 \\ 18.3 \\ -75.2 \\ -163.3 \end{pmatrix}$	$\begin{bmatrix} \{0.58, -0.12, -0.08, 0.80\} \\ \{0.17, 0.84, 0.52, 0.06\} \\ \{0.74, -0.28, 0.28, -0.55\} \\ \{-0.30, -0.46, 0.80, 0.23\} \end{bmatrix}$	$\begin{pmatrix} 12{,}161.0 \\ 12{,}109.7 \\ 12{,}016.3 \\ 11{,}928.2 \end{pmatrix}$	$\begin{pmatrix} 11{,}589.9 \\ 11{,}538.6 \\ 11{,}445.1 \\ 11{,}357.0 \end{pmatrix}$	$\begin{pmatrix} 12{,}444.9 \\ 12{,}393.6 \\ 12{,}300.1 \\ 12{,}212.0 \end{pmatrix}$

Table 8. Rearrangement decays for the $bc\bar{c}\bar{n}$, $bc\bar{c}\bar{s}$, $bc\bar{b}\bar{n}$, and $bc\bar{b}\bar{s}$ states. The numbers in the parentheses are $(100|\mathcal{M}|^2/\mathcal{C}^2, \Gamma)$. The tetraquark mass, partial width Γ, and total width Γ_{sum} values are given in MeV units.

System	J^P	Mass	Decay Channels						Γ_{sum}
$bc\bar{c}\bar{n}$			$B_c^{*-}D^*$	$\bar{B}^*J/\psi$					
	2^+	8713.9	(97.3, 245.8)	(21.8, 55.2)					301.1
		8696.2	(2.1, 5.3)	(77.7, 191.3)					196.6
			$B_c^{*-}D^*$	$B_c^{*-}D$	$B_c^-D^*$	$\bar{B}^*J/\psi$	$\bar{B}^*\eta_c$	$\bar{B}J/\psi$	
	1^+	8719.4	(78.2, 199.0)	(0.1, 0.2)	(2.1, 5.7)	(17.8, 45.6)	(1.2, 3.7)	(10.3, 28.2)	282.3
		8698.4	(19.4, 48.1)	(1.3, 3.8)	(7.6, 20.8)	(79.1, 195.6)	(1.0, 2.8)	(2.1, 5.6)	276.7
		8665.3	(2.1, 4.9)	(1.5, 4.4)	(16.7, 43.9)	(1.2, 2.8)	(3.8, 10.6)	(43.6, 111.1)	177.7
		8633.9	(0.3, 0.6)	(1.0, 2.8)	(64.7, 163.6)	(0.3, 0.8)	(0.1, 0.2)	(38.4, 92.8)	260.6
		8602.3	(0.5, 1.0)	(26.1, 68.7)	(8.4, 20.4)	(0.9, 1.7)	(51.0, 131.6)	(4.8, 10.6)	233.9
		8555.9	(0.1, 0.2)	(69.5, 173.3)	(0.4, 0.8)	(0.4, 0.8)	(42.8, 102.1)	(0.9, 1.7)	278.9
			$B_c^{*-}D^*$	B_c^-D	$\bar{B}^*J/\psi$	$\bar{B}\eta_c$			
	0^+	8746.8	(61.5, 161.5)	(0.1, 0.2)	(49.3, 130.8)	(0.3, 0.8)			293.2
		8668.0	(36.8, 87.5)	(1.2, 3.6)	(45.2, 106.1)	(3.6, 10.8)			208.0
		8572.2	(2.4, 4.8)	(23.4, 65.3)	(4.4, 8.2)	(60.8, 161.9)			240.2
		8478.1	(0.1, 0.1)	(75.9, 190.2)	(1.3, 1.5)	(35.4, 80.0)			271.8
$bc\bar{c}\bar{s}$			$B_c^{*-}D_s^{*+}$	$\bar{B}_s^{*0}J/\psi$					
	2^+	8805.0	(97.3, 240.1)	(21.8, 54.3)					294.3
		8788.1	(2.1, 5.2)	(77.7, 188.5)					193.7
			$B_c^{*-}D_s^{*+}$	$B_c^{*-}D_s^+$	$B_c^-D_s^{*+}$	$\bar{B}_s^{*0}J/\psi$	$\bar{B}_s^{*0}\eta_c$	$\bar{B}_s^0J/\psi$	
	1^+	8811.3	(76.2, 189.5)	(0.1, 0.4)	(2.3, 6.2)	(21.3, 53.7)	(1.3, 3.7)	(9.1, 24.8)	278.1
		8789.2	(23.2, 56.1)	(1.3, 3.8)	(8.1, 21.7)	(75.9, 184.6)	(1.3, 3.6)	(2.3, 6.1)	276.0
		8755.6	(1.4, 3.3)	(1.7, 4.8)	(20.7, 53.2)	(1.3, 3.0)	(3.7, 10.4)	(39.0, 98.0)	172.6
		8722.4	(0.3, 0.6)	(0.7, 1.8)	(61.6, 151.7)	(0.3, 0.7)	(0.3, 0.8)	(42.2, 100.6)	256.1
		8693.8	(0.5, 1.0)	(24.9, 64.6)	(7.1, 16.9)	(0.9, 1.7)	(52.6, 133.4)	(5.7, 12.8)	230.4
		8644.8	(0.1, 0.1)	(72.3, 176.0)	(0.2, 0.4)	(0.4, 0.7)	(41.4, 96.7)	(1.1, 2.1)	276.1
			$B_c^{*-}D_s^{*+}$	$B_c^-D_s^+$	$\bar{B}_s^{*0}J/\psi$	$\bar{B}_s^0\eta_c$			
	0^+	8839.6	(60.1, 154.6)	(0.1, 0.2)	(50.5, 132.3)	(0.2, 0.7)			287.8
		8757.5	(37.7, 87.0)	(1.1, 3.3)	(44.3, 102.0)	(3.8, 11.1)			203.3
		8661.5	(2.4, 4.7)	(24.4, 66.7)	(4.4, 8.0)	(59.3, 155.5)			234.8
		8565.4	(0.1, 0.1)	(74.3, 181.2)	(1.2, 1.3)	(36.5, 81.0)			263.7

Table 8. *Cont.*

System	J^P	Mass	Decay Channels						Γ_{sum}
$bc\bar{b}\bar{n}$			ΥD^*	$\bar{B}^* B_c^{*+}$					
	2^+	12,042.0 12,013.5	(98.5, 174.4) (1.9, 3.3)	(21.3, 38.6) (79.1, 138.6)					213.0 141.9
			ΥD^*	ΥD	$\eta_b D^*$	$\bar{B}^* B_c^{*+}$	$\bar{B}^* B_c^+$	$\bar{B} B_c^{*+}$	
	1^+	12,042.1 12,023.1 11,987.3 11,973.2 11,947.5 11,897.5	(98.4, 174.3) (1.0, 1.8) (0.4, 0.7) (0.0, 0.0) (0.2, 0.4) (0.0, 0.0)	(0.0, 0.0) (0.5, 1.0) (1.9, 3.5) (0.2, 0.4) (1.1, 2.0) (96.1, 169.5)	(0.0, 0.0) (8.6, 15.8) (32.1, 57.9) (50.7, 90.2) (9.3, 16.2) (0.0, 0.0)	(1.3, 2.3) (93.5, 165.9) (3.2, 5.3) (0.4, 0.7) (0.2, 0.3) (1.9, 2.7)	(2.8, 5.5) (0.1, 0.2) (8.3, 15.5) (1.0, 1.8) (77.7, 138.2) (9.7, 16.1)	(5.9, 11.3) (1.4, 2.7) (21.3, 38.5) (57.9, 102.7) (7.5, 12.8) (5.8, 9.3)	193.5 187.4 121.4 195.8 169.9 197.6
			ΥD^*	$\eta_b D$	$\bar{B}^* B_c^{*+}$	$\bar{B} B_c^+$			
	0^+	12,059.3 12,008.3 11,918.1 11,829.5	(68.2, 122.4) (28.7, 49.5) (2.2, 3.5) (0.0, 0.0)	(0.0, 0.0) (0.5, 0.9) (9.5, 17.9) (90.5, 160.6)	(41.0, 76.0) (51.7, 89.9) (4.4, 6.6) (3.1, 3.8)	(0.3, 0.7) (3.6, 7.2) (75.9, 138.5) (19.9, 31.9)			199.2 147.5 166.4 196.3
$bc\bar{b}\bar{s}$			ΥD_s^{*+}	$\bar{B}_s^{*0} B_c^{*+}$					
	2^+	12,143.3 12,114.9	(97.8, 172.9) (2.6, 4.4)	(23.1, 42.1) (77.2, 135.9)					215.0 140.3
			ΥD_s^{*+}	ΥD_s^+	$\eta_b D_s^{*+}$	$\bar{B}_s^{*0} B_c^{*+}$	$\bar{B}_s^{*0} B_c^+$	$\bar{B}_s^0 B_c^{*+}$	
	1^+	12,143.3 12,124.9 12,087.7 12,072.2 12,048.7 11,996.6	(98.4, 173.9) (1.1, 1.9) (0.4, 0.6) (0.0, 0.0) (0.3, 0.6) (0.0, 0.0)	(0.0, 0.0) (0.6, 1.2) (1.9, 3.5) (0.4, 0.8) (0.8, 1.5) (96.3, 169.7)	(0.0, 0.0) (8.5, 15.7) (38.0, 68.3) (44.6, 79.1) (8.0, 14.0) (0.0, 0, 0)	(1.3, 2.3) (92.8, 165.2) (2.8, 4.7) (0.5, 0.8) (0.1, 0.2) (1.8, 2.6)	(3.3, 6.5) (0.1, 0.2) (8.5, 15.9) (2.4, 4.4) (77.4, 138.1) (8.4, 14.0)	(5.2, 10.1) (1.3, 2.4) (15.4, 27.9) (62.5, 111.4) (9.7, 16.7) (5.9, 9.5)	192.9 186.6 120.9 196.5 171.1 195.4
			ΥD_s^{*+}	$\eta_b D_s^+$	$\bar{B}_s^{*0} B_c^{*+}$	$\bar{B}_s^0 B_c^+$			
	0^+	12,161.0 12,109.7 12,016.3 11,928.2	(68.2, 122.2) (29.3, 50.3) (2.2, 3.5) (0.0, 0, 1)	(0.0, 0.0) (0.4, 0.8) (10.0, 18.8) (88.8, 157.2)	(41.0, 76.2) (52.4, 91.5) (4.0, 6.1) (3.0, 3.7)	(0.3, 0.7) (3.5, 7.0) (76.3, 139.5) (20.7, 33.5)			199.2 149.7 168.0 194.5

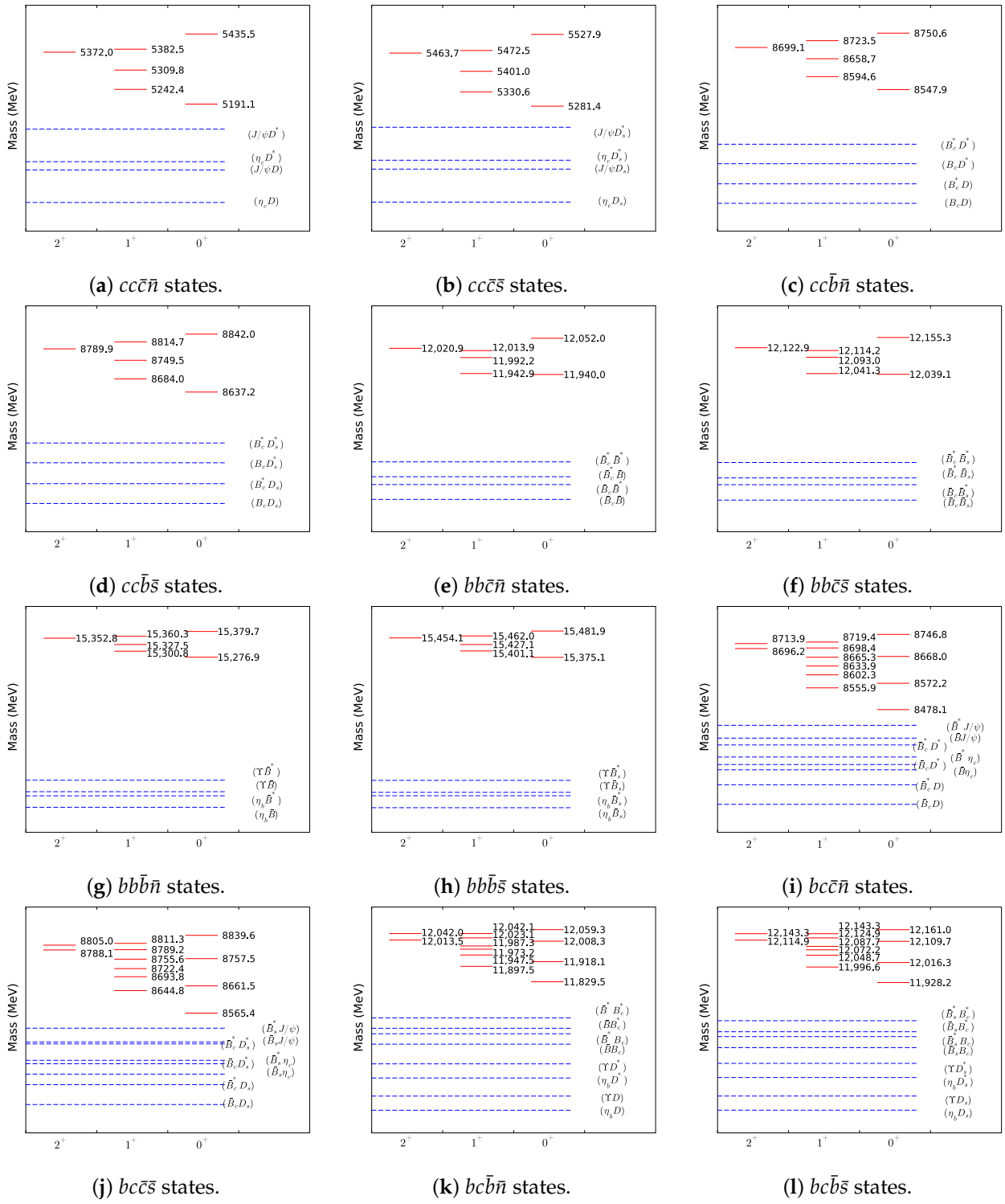

(**a**) $cc\bar{c}\bar{n}$ states. (**b**) $cc\bar{c}\bar{s}$ states. (**c**) $cc\bar{b}\bar{n}$ states.

(**d**) $cc\bar{b}\bar{s}$ states. (**e**) $bb\bar{c}\bar{n}$ states. (**f**) $bb\bar{c}\bar{s}$ states.

(**g**) $bb\bar{b}\bar{n}$ states. (**h**) $bb\bar{b}\bar{s}$ states. (**i**) $bc\bar{c}\bar{n}$ states.

(**j**) $bc\bar{c}\bar{s}$ states. (**k**) $bc\bar{b}\bar{n}$ states. (**l**) $bc\bar{b}\bar{s}$ states.

Figure 1. Relative positions of the triply heavy tetraquark states and their rearrangement decay channels.

3.2. The $cc\bar{c}\bar{n}$, $cc\bar{c}\bar{s}$, $cc\bar{b}\bar{n}$, and $cc\bar{b}\bar{s}$ States

The CMI matrices and their eigenvalues and corresponding eigenvectors, as well as the masses calculated using Equations (2)–(4), for these four tetraquark systems are given in Table 3. The masses calculated using $X(4140)$ as the reference state were our predicted values. The relative positions of these $cc\bar{Q}\bar{q}$ states and related decay channels are illustrated in Figure 1a–d. For the lower limits calculation, several meson–meson thresholds could be adopted. We used the thresholds of $J/\psi D$, $J/\psi D_s$, $B_c D$, and $B_c D_s$ for $cc\bar{c}\bar{n}$, $cc\bar{c}\bar{s}$, $cc\bar{b}\bar{n}$, and $cc\bar{b}\bar{s}$, respectively. Other choices did not affect much. The tetraquark mass upper and lower

limits in Table 3 are consistent with the results in [59], but the obtained masses used in the following discussions were between the upper and lower limits. Due to the values being larger than those in [59], we found no stable tetraquarks in these systems, while stable 2^+ $cc\bar{Q}\bar{q}$ states were found to be possible in [59]. The relevant rearrangement decay channels, corresponding partial widths, and total widths are listed in Table 4.

The $cc\bar{c}\bar{n}$ system had six states, whose masses ranged from 5191.1 to 5435.5 MeV. The highest and lowest tetraquarks were both $J^P = 0^+$ states, and they could decay into the same channels: $J/\psi D^*$ and $\eta_c D$. The rearrangement decays of the higher and lower 0^+ states were dominated by the $J/\psi D^*$ and $\eta_c D$ channels, respectively. There were three 1^+ tetraquarks located from 5242.4 to 5382.5 MeV, with $J/\psi D^*$, $J/\psi D$, and $\eta_c D^*$ as their rearrangement decay modes. The highest state mainly decayed into $J/\psi D^*$. Both the intermediate and lowest states had two dominant channels, namely, $J/\psi D$ and $\eta_c D^*$, but the $\Gamma_{J/\psi D} : \Gamma_{\eta_c D^*}$ ratios were different. Their predicted values were about 0.5 and 1.8, respectively. The 2^+ state was located at 5372.0 MeV, with only one decay mode $J/\psi D^*$ when only the S-wave channel was considered. When the D-wave decays were also counted, it could also decay into $\eta_c D^*$, $J/\psi D$, and $\eta_c D$.

The $cc\bar{b}\bar{n}$ tetraquarks spanned a range from 8547.9 to 8750.6 MeV, with the J^P of the highest and lowest states being 0^+. The two 0^+ tetraquarks had $B_c^* D^*$ and $B_c D$ decay channels. The higher state had a dominant $B_c^* D^*$ decay mode, while the lower state mainly decayed into $B_c D$. Three 1^+ tetraquarks were located in the range of 8594.6∼8723.5 MeV. The dominant decay channels for the highest, intermediate, and lowest states were $B_c^* D^*$, $B_c D^*$, and $B_c^* D$, respectively. The 2^+ state was located around 8700 MeV and should mainly decay into $B_c^* D^*$ via an S-wave interaction, but the three other suppressed D-wave channels $B_c D^*$, $B_c^* D$, and $B_c D$ were also allowed.

When comparing the results for the $cc\bar{c}\bar{s}$ states with those for $cc\bar{c}\bar{n}$, we found that they had almost the same eigenvalues, eigenvectors, and decay information. The $cc\bar{c}\bar{s}$ tetraquarks were about 90 MeV higher than the corresponding $cc\bar{c}\bar{n}$ states, while the decay widths of $cc\bar{c}\bar{s}$ were slightly smaller than those of the corresponding $cc\bar{c}\bar{n}$. The above features were also observed in the $cc\bar{b}\bar{n}$ and $cc\bar{b}\bar{s}$ cases. For the $cc\bar{c}\bar{s}$ ($cc\bar{b}\bar{s}$) tetraquarks, the dominant decay channels were nearly the same as those of $cc\bar{c}\bar{n}$ ($cc\bar{b}\bar{n}$), except for replacing $D^{(*)}$ in the final states with $D_s^{(*)}$.

3.3. The $bb\bar{c}\bar{n}$, $bb\bar{c}\bar{s}$, $bb\bar{b}\bar{n}$, and $bb\bar{b}\bar{s}$ States

We list the CMI- and tetraquark-mass-related results for the $bb\bar{Q}\bar{q}$ states in Table 5. The relative positions with masses using $X(4140)$ as the reference state are illustrated in Figure 1e–h. For the lower limit calculations with Equation (3), the meson–meson thresholds that we chose were those of $B_c^- \bar{B}$, $B_c^- \bar{B}_s^0$, $\Upsilon\bar{B}$, and $\Upsilon\bar{B}_s^0$ for $bb\bar{c}\bar{n}$, $bb\bar{c}\bar{s}$, $bb\bar{b}\bar{n}$, and $bb\bar{b}\bar{s}$, respectively. We obtained values of the lower limits (and upper limits with Equation (2)) similar to those in [59]. The masses predicted in this study were between the lower and upper limits. Due to the higher spectra (see Figure 1), no stable tetraquark states existed in the $bb\bar{Q}\bar{q}$ systems. We present the relevant rearrangement decay channels, corresponding partial widths, and total widths in Table 6.

The $bb\bar{c}\bar{n}$ tetraquarks were distributed in the 11,940.0∼12,052.0 MeV mass range, with the J^P of both the highest and lowest states being 0^+. The two 0^+ states could both decay into $\bar{B}_c^* \bar{B}^*$ and $\bar{B}_c \bar{B}$ (here, we simply use $\bar{B}_c^{(*)}$ and $\bar{B}_s^{(*)}$ to denote $B_c^{(*)-}$ and $\bar{B}_s^{(*)0}$, respectively). The former (latter) channel was dominant for the higher (lower) tetraquark. There were three 1^+ states that ranged from 11,942.9 to 12,013.9 MeV, with three decay

channels: $\bar{B}_c^*\bar{B}^*$, $\bar{B}_c^*\bar{B}$, and $\bar{B}_c\bar{B}^*$. The respective partial width ratios of the dominant decay channels for the highest, intermediate, and lowest 1^+ states were

$$\begin{aligned} \Gamma_{\bar{B}_c^*\bar{B}^*} : \Gamma_{\bar{B}_c^*\bar{B}} &= 4.5, \\ \Gamma_{\bar{B}_c^*\bar{B}^*} : \Gamma_{\bar{B}_c^*\bar{B}} : \Gamma_{\bar{B}_c\bar{B}^*} &= 1.0 : 4.8 : 3.6, \\ \Gamma_{\bar{B}_c^*\bar{B}} : \Gamma_{\bar{B}_c\bar{B}^*} &= 0.5. \end{aligned} \tag{13}$$

The 2^+ state was located around 12.0 GeV, with only one S-wave decay channel: $\bar{B}_c^*\bar{B}^*$. The other three channels, namely, $\bar{B}_c^*\bar{B}$, $\bar{B}_c\bar{B}^*$, and $\bar{B}_c\bar{B}$, were also allowed if the D-wave decays were counted.

Like the discussion in the above $cc\bar{Q}\bar{q}$ case, we compared the $bb\bar{c}\bar{s}$ results with the $bb\bar{c}\bar{n}$ results and found similar features. Our estimation indicated that the $bb\bar{c}\bar{s}$ tetraquarks were about 100 MeV heavier than the $bb\bar{c}\bar{n}$ states, but they had comparable widths. By replacing $\bar{B}^{(*)}$ with $\bar{B}_s^{(*)}$ in the final states, we obtained the decay channels of the $bb\bar{c}\bar{s}$ tetraquarks from those of the $bb\bar{c}\bar{n}$ states. The main decay channel was $\bar{B}_c^*\bar{B}_s^*$ for the higher 0^+ $bb\bar{c}\bar{s}$, while it was $\bar{B}_c\bar{B}_s$ for the lower one. The partial width ratios of the dominant channels for the highest, intermediate, and lowest 1^+ $bb\bar{c}\bar{s}$ tetraquarks were $\Gamma_{\bar{B}_c^*\bar{B}_s^*} : \Gamma_{\bar{B}_c^*\bar{B}_s} = 5.1$, $\Gamma_{\bar{B}_c^*\bar{B}_s^*} : \Gamma_{\bar{B}_c^*\bar{B}_s} : \Gamma_{\bar{B}_c\bar{B}_s^*} = 1.0 : 6.4 : 5.3$, and $\Gamma_{\bar{B}_c^*\bar{B}_s} : \Gamma_{\bar{B}_c\bar{B}_s^*} = 0.6$, respectively. The 2^+ $bb\bar{c}\bar{s}$ tetraquark could decay into $\bar{B}_c^*\bar{B}_s^*$ through S-wave interactions, but it also had the suppressed D-wave decay channels $\bar{B}_c^*\bar{B}_s$, $\bar{B}_c\bar{B}_s^*$, and $\bar{B}_c\bar{B}_s$.

The $bb\bar{b}\bar{n}$ tetraquarks were distributed in the range of 15,276.9∼15,379.7 MeV. The two 0^+ states had the decay channels $\Upsilon\bar{B}^*$ and $\eta_b\bar{B}$, with the former (latter) being dominant for the higher (lower) tetraquark. The 1^+ tetraquark states had three decay channels. The highest 1^+ state mainly decayed into $\Upsilon\bar{B}^*$, while the other two mainly decayed into $\Upsilon\bar{B}$ and $\eta_b\bar{B}^*$. The partial width ratios of the dominant channels for the intermediate and lowest states were $\Gamma_{\Upsilon\bar{B}} : \Gamma_{\eta_b\bar{B}^*} = 3.0$ and 0.4, respectively. The 2^+ tetraquark had one S-wave channel $\Upsilon\bar{B}^*$ and three suppressed D-wave channels.

As for the $bb\bar{b}\bar{s}$ tetraquarks, the decay channels could be obtained from the $bb\bar{b}\bar{n}$ states by replacing $\bar{B}^{(*)}$ with $\bar{B}_s^{(*)}$ in the final states. The partial width ratios of the dominant channels for the intermediate and lowest 1^+ $bb\bar{b}\bar{s}$ tetraquarks were $\Gamma_{\Upsilon\bar{B}_s} : \Gamma_{\eta_b\bar{B}_s^*} = 2.3$ and 0.5, respectively.

3.4. The $bc\bar{c}\bar{n}$, $bc\bar{c}\bar{s}$, $bc\bar{b}\bar{n}$, and $bc\bar{b}\bar{s}$ States

The Pauli principle does not place constraints on the tetraquark wave functions, and the total number of states in each system was twelve. We present the CMI- and tetraquark-mass-related results in Table 7 and plot the mass spectra using $X(4140)$ as the reference state in Figure 1i–l. When obtaining the lower limits for the tetraquark masses in Table 7, we adopted the meson–meson thresholds of B_c^-D, $B_c^-D_s^+$, ΥD, and ΥD_s^+ for the $bc\bar{c}\bar{n}$, $bc\bar{c}\bar{s}$, $bc\bar{b}\bar{n}$, and $bc\bar{b}\bar{s}$ systems, respectively. Similar values for the lower and upper limits can be found in [59]. For these $bc\bar{Q}\bar{q}$ systems, an alternative selection of reference meson–meson states is possible. When the meson–meson thresholds of $\bar{B}J/\psi$, $\bar{B}_sJ/\psi$, $\bar{B}B_c$, and $\bar{B}_sB_c$ were used to estimate the tetraquark masses in [59], values larger than the lower limits were obtained, but they were smaller than the predicted values that we obtained here. Our $bc\bar{Q}\bar{q}$ tetraquark masses were smaller than the upper limits. As shown in Figure 1, more rearrangement decay channels existed than in the previous cases, and all the $bc\bar{Q}\bar{q}$ tetraquarks were unstable. Table 8 lists the decay information in our scheme. One may calculate the partial width ratios of different channels for a given tetraquark using this table.

The $bc\bar{c}\bar{n}$ tetraquarks had masses that ranged from 8478.1 to 8746.8 MeV. For the highest and second-highest 0^+ states, the dominant channel partial width ratios were

$\Gamma_{\bar{B}_c^* D^*} : \Gamma_{\bar{B}^* J/\psi} = 1.2$ and 0.8, respectively. For the second-lowest and lowest 0^+ states, these were $\Gamma_{\bar{B}_c D} : \Gamma_{\bar{B}\eta_c} = 0.4$ and 2.3, respectively. There were six 1^+ $bc\bar{c}\bar{n}$ tetraquarks. From the highest to lowest, the partial width ratios of their dominant channels were

$$\begin{aligned}
\Gamma_{B_c^{*-} D^*} : \Gamma_{\bar{B}^* J/\psi} : \Gamma_{\bar{B} J/\psi} &= 7.1 : 1.6 : 1.0, \\
\Gamma_{B_c^{*-} D^*} : \Gamma_{B_c^- D^*} : \Gamma_{\bar{B}^* J/\psi} &= 2.3 : 1.0 : 9.4, \\
\Gamma_{B_c^- D^*} : \Gamma_{\bar{B}^* \eta_c} : \Gamma_{\bar{B} J/\psi} &= 4.1 : 1.0 : 10.5, \\
\Gamma_{B_c^- D^*} : \Gamma_{\bar{B} J/\psi} &= 1.8, \\
\Gamma_{B_c^{*-} D} : \Gamma_{B_c^- D^*} : \Gamma_{\bar{B}^* \eta_c} : \Gamma_{\bar{B} J/\psi} &= 6.5 : 1.9 : 12.4 : 1.0, \\
\Gamma_{B_c^{*-} D} : \Gamma_{\bar{B}^* \eta_c} &= 1.7.
\end{aligned} \tag{14}$$

For the S-wave decays of the two 2^+ tetraquarks, the higher state had a partial width ratio of $\Gamma_{\bar{B}_c^* D^*} : \Gamma_{\bar{B}^* J/\psi} = 4.4$, while the lower one mainly decayed into $\bar{B}^* J/\psi$.

The twelve $bc\bar{c}\bar{s}$ tetraquark masses were about 90 MeV heavier than those of the $bc\bar{c}\bar{n}$ states. We easily obtained their S-wave decay channels from the $bc\bar{c}\bar{n}$ states by replacing an n quark with an s quark in the final states. The rearrangement decay properties of these two systems had similar features.

The $bc\bar{b}\bar{n}$ tetraquarks were located in the 11,829.5∼12,059.3 MeV mass range, and the $bc\bar{b}\bar{s}$ states were about 100 MeV heavier. These two systems' rearrangement decays were also similar.

4. Discussion and Summary

Similar to fully heavy tetraquark states, a triply heavy tetraquark's exotic nature is easy to identify. In this work, we studied the spectra of triply heavy tetraquark states in a modified CMI model using a diquark–antidiquark base, with the assumption that $X(4140)$ was the lowest 1^{++} compact $cs\bar{c}\bar{s}$ tetraquark state. Two-body strong decays were also studied in a simple rearrangement decay scheme. We temporarily estimated the widths by adopting the decay parameter extracted from the width of $X(6600)$, which is considered a fully charmed compact tetraquark.

The 12 considered systems involved 96 states in total. Some tetraquarks had very similar masses, posing challenges in distinguishing them based solely on the spectrum. Fortunately, their dominant two-body decay channels and the corresponding partial width ratios were different. Therefore, the structures of exotic states could be identified by their measured masses, quantum numbers, and/or strong decay properties.

For calculations with the original CMI model, 14 coupling parameters and 4 quark masses that were extracted from the conventional hadron masses were adopted. However, these parameters may introduce considerable uncertainty to tetraquark masses because of differences in the inner structures and interactions between conventional hadrons and compact tetraquark states. Since the values of the effective quark masses are much larger than those of the effective coupling constants, the quark masses predominate this uncertainty. To reduce the uncertainty, we introduced modified mass formulae using hadron–hadron states and multiquark candidates as references [59,73,74]. With these methods, we obtained lower and more reasonable numerical results than the original CMI model. However, we have not yet considered the uncertainty from coupling parameters C_{ij}. They are hard to derive from fundamental theories. Their extraction from tetraquark states is also impossible due to the lack of awareness of exotic hadrons. The coupling parameter uncertainties are difficult to reduce right now and, thus, should be studied in future works.

To study the dominant two-body strong decays of triply heavy tetraquark states, we introduced a simple rearrangement scheme by assuming that the Hamiltonian governing

the decay processes was a constant parameter. Since there has been no observed triply heavy tetraquark candidate yet, we temporarily used the parameter extracted from the width of the possible fully charmed tetraquark $X(6600)$ and estimated each channel's partial decay width for all the studied tetraquark states. Note that each system should have a unique decay parameter, and, thus, the adopted assumption is very crude. The numerical results that we present may be very different from the real values. However, the different channels' partial width ratios may rarely be dependent on this parameter and offer valuable information to understand exotic state structures.

In Section 2.1, we consider the tetraquark masses estimated with Equation (2) as theoretical upper limits. Here, we introduce another method to constrain the upper limits. Suppose that there is a triply heavy hexaquark state $QQq\bar{Q}\bar{q}\bar{q}$; we can estimate its mass by using Equation (3) with two reference hadron–hadron states $QQ\bar{Q}\bar{q} + q\bar{q}$ and $QQq + \bar{Q}\bar{q}\bar{q}$. Previous experience [74,75,78,84] suggests that the estimated mass of a multiquark state with a reference system containing one heavy hadron and one light hadron is lighter than that with a reference system consisting of two heavy hadrons; thus, one obtains the hexaquark mass relation $M_1 < M_2$, where

$$\begin{aligned} M_1 &= [M_{QQ\bar{Q}\bar{q}} - (E_{CMI})_{QQ\bar{Q}\bar{q}}] + [M_{q\bar{q}} - (E_{CMI})_{q\bar{q}}] + (E_{CMI})_{QQq\bar{Q}\bar{q}\bar{q}}, \\ M_2 &= [M_{QQq} - (E_{CMI})_{QQq}] + [M_{\bar{Q}\bar{q}\bar{q}} - (E_{CMI})_{\bar{Q}\bar{q}\bar{q}}] + (E_{CMI})_{QQq\bar{Q}\bar{q}\bar{q}}. \end{aligned} \tag{15}$$

Setting $M_1 = M_2$ may constrain the upper limit for the $QQ\bar{Q}\bar{q}$ mass. Here, we just considered the case $QQq \to \Xi_{cc}$ because it is currently the only observed doubly heavy baryon. Then, the formula to constrain the upper limit reads as

$$\begin{aligned} M^{upper}_{cc\bar{Q}\bar{q}} &= [M_{\Xi_{cc}} - (E_{CMI})_{\Xi_{cc}}] - [M_{n\bar{q}'} - (E_{CMI})_{n\bar{q}'}] \\ &\quad + [M_{\bar{Q}\bar{q}\bar{q}'} - (E_{CMI})_{\bar{Q}\bar{q}\bar{q}'}] + (E_{CMI})_{cc\bar{Q}\bar{q}}. \end{aligned} \tag{16}$$

Considering different meson and baryon states, we obtained the minimum values for $M^{upper}_{cc\bar{Q}\bar{q}}$, which are collected in Table 9. Here, we chose to use K for the light meson and Ξ_c, Ω_c, Ξ_b, and Ω_b for the baryons in the $cc\bar{c}\bar{n}$, $cc\bar{c}\bar{s}$, $cc\bar{b}\bar{n}$, and $cc\bar{b}\bar{s}$ cases, respectively. Compared with Table 3, the values in Table 9 are smaller than the upper limits but higher than the masses predicted using $X(4140)$ as the reference. Therefore, the updated upper limits were reasonable, and the measured $cc\bar{Q}\bar{q}$ tetraquarks beyond these constraints should be interpreted as excited states. Note that it would be possible to obtain new constraints from the Ω_{cc} mass if it were observed.

Table 9. Upper limits for the masses of $cc\bar{Q}\bar{q}$ states estimated with Equation (16) in MeV units.

J^P \ System	$cc\bar{c}\bar{n}$	$cc\bar{c}\bar{s}$	$cc\bar{b}\bar{n}$	$cc\bar{b}\bar{s}$
2^+	5477.7	5638.8	8793.2	8944.1
1^+	5488.2 5415.5 5348.1	5647.7 5576.2 5505.8	8817.6 8752.8 8688.8	8968.9 8903.7 8838.2
0^+	5541.3 5296.9	5703.1 5456.5	8844.8 8642.0	8996.1 8791.4

In the above discussions, we introduce a reference system to reduce the mass uncertainty for tetraquark states from effective quark masses. The uncertainties are now governed by those of the quark mass gaps Δ_{ij}. Their effects are easy to see from the mass formula (5). It is clear that the uncertainties of the coupling parameters C_{ij} also affect the estimated values. We move on to this issue. Because of the complicated quark couplings in

tetraquark structures, the properties of two-quark interactions become unclear. To reflect the effects induced by small variations in the coupling parameters, a dimensionless constant

$$K_{ij} = \frac{\partial E_{CMI}}{\partial C_{ij}}, \tag{17}$$

can be defined [45,73,85]. With this constant, the CMI eigenvalue can be written as

$$E_{CMI} = \sum_{i<j} K_{ij} C_{ij}. \tag{18}$$

One should note that this formula (18) does not mean that E_{CMI} is the linear superposition of the C_{ij}s because the value of K_{ij} also relies on C_{ij}. With the K_{ij} amplitudes, one can roughly understand the influence that the coupling parameters C_{ij} have on the estimated tetraquark masses. The K_{ij} values that we calculated are listed in Tables 10–12. The results show that the effect on the tetraquark masses due to the uncertainty of C_{ij} depends on the states. For example, the uncertainties of C_{cc}, $C_{c\bar{c}}$, $C_{c\bar{n}}$, and C_{cn} had equal effects on the 2^+ $cc\bar{c}\bar{n}$ state mass, while those of $C_{c\bar{c}}$ and $C_{c\bar{n}}$ had larger effects on the ground 0^+ $cc\bar{c}\bar{n}$ than C_{cc} and C_{cn} did. As for the tetraquark mass uncertainties, they could even be tens of MeV if those of $C_{c\bar{c}}$ and $C_{c\bar{n}}$ are both 1 MeV. It was also observed that the effects in the n and s cases were not so different.

Table 10. K factors of CMI eigenvalues for $cc\bar{c}\bar{n}$, $cc\bar{c}\bar{s}$, $cc\bar{b}\bar{n}$, and $cc\bar{b}\bar{s}$ states.

System	J^P	Mass	K Factors				System	J^P	Mass	K Factors			
$cc\bar{c}\bar{n}$			K_{cc}	$K_{c\bar{c}}$	$K_{c\bar{n}}$	K_{cn}	$cc\bar{c}\bar{s}$			K_{cc}	$K_{c\bar{c}}$	$K_{c\bar{s}}$	K_{cs}
	2^+	5372.0	2.7	2.7	2.7	2.7		2^+	5463.7	2.7	2.7	2.7	2.7
	1^+	5382.5	3.5	4.9	6.0	−3.9		1^+	5472.5	3.5	4.8	6.0	−3.8
		5309.8	2.7	−4.6	−0.8	2.4			5401.0	2.7	−4.5	−0.8	2.3
		5242.4	3.2	−3.0	−7.9	−5.2			5330.6	3.2	−3.0	−7.9	−5.2
	0^+	5435.5	3.5	7.5	7.5	3.5		0^+	5527.9	3.5	7.5	7.5	3.5
		5191.1	3.1	−12.8	−12.8	3.1			5281.4	3.1	−12.8	−12.8	3.1
$cc\bar{b}\bar{n}$			K_{cc}	$K_{b\bar{c}}$	$K_{c\bar{n}}$	K_{bn}	$cc\bar{b}\bar{s}$			K_{cc}	$K_{b\bar{c}}$	$K_{c\bar{s}}$	K_{bs}
	2^+	8699.1	2.7	2.7	2.7	2.7		2^+	8789.9	2.7	2.7	2.7	2.7
	1^+	8723.5	3.4	4.2	6.5	−3.9		1^+	8814.7	3.4	4.1	6.5	−3.9
		8658.7	2.7	−8.7	2.7	0.3			8749.5	2.7	−8.7	2.7	0.3
		8594.6	3.2	1.9	−11.9	−3.1			8684.0	3.2	1.9	−11.9	−3.1
	0^+	8750.6	3.5	7.5	7.5	3.5		0^+	8842.0	3.5	7.5	7.5	3.5
		8547.9	3.1	−12.8	−12.8	3.1			8637.2	3.1	−12.8	−12.8	3.1

Table 11. K factors of CMI eigenvalues for $bb\bar{c}\bar{n}$, $bb\bar{c}\bar{s}$, $bb\bar{b}\bar{n}$, and $bb\bar{b}\bar{s}$ states.

System	J^P	Mass	K Factors				System	J^P	Mass	K Factors			
$bb\bar{c}\bar{n}$			K_{bb}	$K_{b\bar{c}}$	$K_{b\bar{n}}$	K_{cn}	$bb\bar{c}\bar{s}$			K_{bb}	$K_{b\bar{c}}$	$K_{b\bar{s}}$	K_{cs}
	2^+	12,020.9	2.7	2.7	2.7	2.7		2^+	12,122.9	2.7	2.7	2.7	2.7
	1^+	12,013.9	3.6	7.0	1.8	−2.6		1^+	12,114.2	3.6	6.8	2.3	−2.7
		11,992.2	2.7	−1.9	−2.0	1.7			12,093.0	2.7	−2.2	−2.0	2.0
		11,942.9	3.1	−7.8	−2.4	−5.7			12,041.3	3.0	−7.2	−3.0	−5.9
	0^+	12,052.0	3.6	7.5	7.5	3.6		0^+	12,155.3	3.6	7.5	7.5	3.6
		11,940.0	3.1	−12.8	−12.8	3.1			12,039.1	3.1	−12.8	−12.8	3.1
$bb\bar{b}\bar{n}$			K_{bb}	$K_{b\bar{b}}$	$K_{b\bar{n}}$	K_{bn}	$bb\bar{b}\bar{s}$			K_{bb}	$K_{b\bar{b}}$	$K_{b\bar{s}}$	K_{bs}
	2^+	15,352.8	2.7	2.7	2.7	2.7		2^+	15,454.1	2.7	2.7	2.7	2.7
	1^+	15,360.3	3.5	6.2	4.8	−3.9		1^+	15,462.0	3.5	6.0	5.0	−4.0
		15,327.5	2.7	0.4	−5.9	2.0			15,427.1	2.7	−0.2	−5.2	2.3
		15,300.8	3.2	−9.2	−1.6	−4.8			15,401.1	3.2	−8.4	−2.5	−5.0
	0^+	15,379.7	3.5	7.5	7.5	3.5		0^+	15,481.9	3.5	7.5	7.5	3.5
		15,276.9	3.1	−12.8	−12.8	3.1			15,375.1	3.1	−12.8	−12.8	3.1

Table 12. K factors of CMI eigenvalues for $bc\bar{c}\bar{n}$, $bc\bar{c}\bar{s}$, $bc\bar{b}\bar{n}$, and $bc\bar{b}\bar{s}$ states.

System	J^P	Mass	K Factors					
$bc\bar{c}\bar{n}$			K_{bc}	$K_{b\bar{c}}$	$K_{b\bar{n}}$	$K_{c\bar{c}}$	$K_{c\bar{n}}$	K_{cn}
	2^+	8713.9	−0.5	5.2	0.7	0.7	5.2	−0.5
		8696.2	1.9	−0.5	4.0	4.0	0.5	1.9
	1^+	8719.4	−2.6	3.8	−0.5	2.1	4.6	2.8
		8698.4	2.7	0.3	4.2	4.2	1.7	−2.7
		8665.3	0.1	−1.8	−6.0	1.6	0.7	2.5
		8633.9	1.0	−10.5	−6.4	2.4	3.4	−3.9
		8602.3	−3.3	−0.2	1.7	−7.9	−3.8	3.0
		8555.9	0.8	3.8	2.3	−7.0	−11.3	−3.1
	0^+	8746.8	3.5	4.0	3.5	3.5	4.0	3.5
		8668.0	−5.9	2.6	2.3	2.3	2.6	−5.9
		8572.2	2.7	−3.7	−9.2	−9.2	−3.7	2.7
		8478.1	−3.0	−12.2	−5.9	−5.9	−12.2	−3.0
$bc\bar{c}\bar{s}$			K_{bc}	$K_{b\bar{c}}$	$K_{b\bar{s}}$	$K_{c\bar{c}}$	$K_{c\bar{s}}$	K_{cs}
	2^+	8805.0	−0.5	5.2	0.6	0.6	5.2	−0.5
		8788.1	1.9	−0.5	4.0	4.0	−0.5	1.9
	1^+	8811.3	−2.8	3.6	−0.1	2.2	4.5	2.9
		8789.2	2.9	0.4	4.0	4.0	1.9	−2.9
		8755.6	0.2	−2.4	−5.4	1.4	0.8	2.6
		8722.4	0.9	−10.1	−7.0	2.5	3.4	−3.9
		8693.8	−3.3	−0.1	1.7	−8.0	−3.6	3.0
		8644.8	0.8	3.9	2.1	−6.7	−11.5	−3.1
	0^+	8839.6	3.5	3.9	3.5	3.5	3.9	3.5
		8757.5	−5.9	2.6	2.3	2.3	2.6	−5.9
		8661.5	2.8	−3.9	−9.0	−9.0	−3.9	2.8
		8565.4	−3.0	−12.0	−6.1	−6.1	−12.0	−3.0
$bc\bar{b}\bar{n}$			K_{bc}	$K_{b\bar{b}}$	$K_{b\bar{n}}$	$K_{b\bar{c}}$	$K_{c\bar{n}}$	K_{bn}
	2^+	12,042.0	−0.5	5.2	0.6	0.6	5.2	−0.5
		12,013.5	1.8	−0.5	4.1	4.1	−0.5	1.8
	1^+	12,042.1	0.7	5.3	−0.2	0.6	5.2	−1.0
		12,023.1	−0.7	−1.1	4.7	5.1	1.4	0.5
		11,987.3	0.9	−4.0	−2.3	0.0	1.3	2.3
		11,973.2	1.2	−8.2	−9.5	3.0	2.8	−3.5
		11,947.5	−3.0	−1.8	2.9	−12.1	0.0	1.3
		11,897.5	−0.4	5.2	−0.3	−1.2	−15.4	−1.0
	0^+	12,059.3	3.3	4.3	3.2	3.2	4.3	3.3
		12,008.3	−5.8	2.5	2.4	2.4	2.5	−5.8
		11,918.1	1.8	−1.6	−11.8	−11.8	−1.6	1.8
		11,829.5	−2.0	−14.5	−3.2	−3.2	−14.5	−2.0
$bc\bar{b}\bar{s}$			K_{bc}	$K_{b\bar{b}}$	$K_{b\bar{s}}$	$K_{b\bar{c}}$	$K_{c\bar{s}}$	K_{bs}
	2^+	12,143.3	−0.5	5.2	0.7	0.7	5.2	−0.5
		12,114.9	1.9	−0.5	4.0	4.0	−0.5	1.9
	1^+	12,143.3	0.7	5.3	0.0	0.5	5.2	−1.1
		12,124.9	−0.8	−1.1	4.8	5.1	1.4	0.6
		12,087.7	1.0	−5.1	−1.5	−0.3	1.6	2.1
		12,072.2	1.1	−7.3	−10.0	2.9	2.5	−3.1
		12,048.7	−3.0	−1.7	2.6	−11.8	0.0	1.1
		11,996.6	−0.5	5.2	−0.4	−1.1	−15.4	−0.9
	0^+	12,161.0	3.3	4.2	3.2	3.2	4.2	3.3
		12,109.7	−5.9	2.5	2.5	2.5	2.5	−5.9
		12,016.3	1.9	−1.7	−11.7	−11.7	−1.7	1.9
		11,928.2	−2.1	−14.4	−3.3	−3.3	−14.4	−2.1

Our mass predictions relied on the $X(4140)$ state as a 1^{++} reference tetraquark. In previous theoretical works [28,78,79,86,87], $X(4140)$ was regarded as a 1^{++} $cs\bar{c}\bar{s}$ tetraquark. However, this exotic state's inner structure has not been confirmed in experiments, and it is still a subject of theoretical debate. If this state is something other than a tetraquark, one has to consider the effects of this reference assumption on the predictions. For example, a detailed study of $cs\bar{c}\bar{s}$ states in the chiral quark model [88] did not obtain a $cs\bar{c}\bar{s}$ tetraquark that was consistent with the observed $X(4140)$, while the authors of [89] interpreted $X(4140)$ as the charmonium state $\chi_{c1}(3P)$ according to their calculation in a relativistic screened potential model. In this situation, all the tetraquark states' masses would change some of the values in our framework since the mass splittings between the $QQ\bar{Q}\bar{q}$ tetraquark

states remain unaffected. What we need from the adopted assumption is actually the determination of a tetraquark mass (input scale of the approach). If the observed $X(4140)$ is a mixed structure of charmonium, a molecule, and a compact $cs\bar{c}\bar{s}$ tetraquark, one anticipates that the theoretical mass of the compact $cs\bar{c}\bar{s}$ would not be far from the $D_s^{*+}D_s^{*-}$ threshold; otherwise, the mixing would not be significant. As a result, the shifted value would not be very large. This theoretical scale's determination depends on the proportion of the compact $cs\bar{c}\bar{s}$ in the wave function of $X(4140)$. If $X(4140)$ does not contain a $cs\bar{c}\bar{s}$ component, one may determine the shifted value by treating another compact tetraquark candidate as a reference. In [88], the interpretation of $X(4274)$ and $X(4350)$ as ground 1^{++} and 0^{++} $cs\bar{c}\bar{s}$ tetraquarks, respectively, was proposed. If $X(4274)$ is indeed the ground 1^{++} $cs\bar{c}\bar{s}$ and we took its mass as the input scale, our predictions for all the tetraquark masses would shift upward by about $M_{X(4274)} - M_{X(4140)} \approx 140$ MeV.

For exotic hadrons, one has to confirm whether they exist through experimental measurements. Most states that we considered here have the quantum numbers of $D^{(*)}$, $D_s^{(*)}$, $\bar{B}^{(*)}$, or $\bar{B}_s^{(*)}$ but with much higher masses. Such resonances can be searched for in the invariant mass distributions of a heavy quarkonium and a $Q\bar{q}$ meson in high-energy colliders, such as the LHC and future CEPC. The $cc\bar{b}\bar{q}$ and $bb\bar{c}\bar{q}$ states are explicitly exotic, and they can be searched for similarly.

Here, we considered only a simple rearrangement scheme in which the decay appeared to occur through quark component free collisions. In principle, the decay parameter $\mathcal{C}$ may be evaluated with the quark-level wave functions of the initial and final states. The gluon exchange contributions certainly affect the $\mathcal{C}$ value further. Such a contribution can probably be explored in a similar way to the quark interchange model in [90]. Because the $\mathcal{C}$ parameter varies with the state, it is possible that its variation may significantly alter the predicted decay width ratios. However, the spatial wave functions should be obtained for such a consideration. If one wants to include gluon exchange contributions to $\mathcal{C}$ but without explicit spatial wave functions, additional parameters would be introduced, which are not easy to determine with the available experimental data.

Replacing the light antiquark in a triply heavy tetraquark state with a light diquark (triquark) would produce a triply heavy pentaquark (hexaquark) state. The present framework can be extended to study such systems. In the extension, one would confront the problem of how to select appropriate reference scales that are consistent with tetraquark studies. We will consider this problem in future investigations.

To summarize, we studied the properties of triply heavy tetraquark states in this work. We estimated their spectra in a modified CMI model by treating $X(4140)$ as a reference 1^{++} tetraquark. No stable state was found. We also considered their two-body strong decays and the related indicative partial width ratios of different channels in a simple rearrangement scheme. We hope that our results can help future experimental searches for such exotic states.

Author Contributions: Conceptualization, Y.-R.L.; methodology, S.-Y.L., Z.-G.S. and J.W.; validation, Z.-L.M. and J.W.; formal analysis, C.-R.S. and Z.-L.M.; writing—original draft preparation, C.-R.S.; writing—review and editing, Y.-R.L. All authors have read and agreed to the published version of the manuscript.

Funding: This project was supported by the National Natural Science Foundation of China (Nos. 12235008, 12275157, 12475143, 11905114) and the Shandong Province Natural Science Foundation (ZR2023MA041).

Data Availability Statement: No new data were created or analyzed in this study. Data sharing is not applicable to this article.

Acknowledgments: We thank all the members of our particle theory group for their discussions and collaborations.

Conflicts of Interest: The authors declare no conflicts of interest.

References

1. Belle Collaboration. Observation of a narrow charmonium-like state in exclusive $B^{\pm} \to K^{\pm}\pi^{+}\pi^{-}J/\psi$ decays. *Phys. Rev. Lett.* **2003**, *91*, 262001. [CrossRef] [PubMed]
2. Belle Collaboration. Observation of a new charmonium state in double charmonium production in $e^{+}e^{-}$ annihilation at $\sqrt{s} \approx 10.6$ GeV. *Phys. Rev. Lett.* **2007**, *98*, 082001. [CrossRef]
3. Belle Collaboration. Production of New Charmoniumlike States in $e^{+}e^{-} \to J/\psi D^{(*)}\bar{D}^{(*)}$ at $\sqrt{s} \approx 10.6$ GeV. *Phys. Rev. Lett.* **2008**, *100*, 202001. [CrossRef] [PubMed]
4. Belle Collaboration. Observation of a charmonium-like enhancement in the $\gamma\gamma \to \omega J/\psi$ process. *Phys. Rev. Lett.* **2010**, *104*, 092001. [CrossRef] [PubMed]
5. Belle Collaboration. Evidence for a new resonance and search for the Y(4140) in the $\gamma\gamma \to \phi J/\psi$ process. *Phys. Rev. Lett.* **2010**, *104*, 112004. [CrossRef]
6. CDF Collaboration. Evidence for a Narrow Near-Threshold Structure in the $J/\psi\phi$ Mass Spectrum in $B^{+} \to J/\psi\phi K^{+}$ Decays. *Phys. Rev. Lett.* **2009**, *102*, 242002. [CrossRef] [PubMed]
7. LHCb Collaboration. Observation of $J/\psi\phi$ structures consistent with exotic states from amplitude analysis of $B^{+} \to J/\psi\phi K^{+}$ decays. *Phys. Rev. Lett.* **2017**, *118*, 022003. [CrossRef]
8. LHCb Collaboration. Amplitude analysis of $B^{+} \to J/\psi\phi K^{+}$ decays. *Phys. Rev. D* **2017**, *95*, 012002. . [CrossRef]
9. BESIII Collaboration. Precise measurement of the $e^{+}e^{-} \to \pi^{+}\pi^{-}J/\psi$ cross section at center-of-mass energies from 3.77 to 4.60 GeV. *Phys. Rev. Lett.* **2017**, *118*, 092001. [CrossRef]
10. BESIII Collaboration. Evidence of Two Resonant Structures in $e^{+}e^{-} \to \pi^{+}\pi^{-}h_c$. *Phys. Rev. Lett.* **2017**, *118*, 092002. [CrossRef] [PubMed]
11. Belle Collaboration. Observation of an alternative $\chi_{c0}(2P)$ candidate in $e^{+}e^{-} \to J/\psi D\bar{D}$. *Phys. Rev. D* **2017**, *95*, 112003. [CrossRef]
12. LHCb Collaboration. Evidence for an $\eta_c(1S)\pi^{-}$ resonance in $B^{0} \to \eta_c(1S)K^{+}\pi^{-}$ decays. *Eur. Phys. J. C* **2018**, *78*, 1019. [CrossRef]
13. BESIII Collaboration. Observation of a Charged Charmoniumlike Structure in $e^{+}e^{-} \to \pi^{+}\pi^{-}J/\psi$ at $\sqrt{s} = 4.26$ GeV. *Phys. Rev. Lett.* **2013**, *110*, 252001. [CrossRef]
14. Belle Collaboration. Study of $e^{+}e^{-} \to \pi^{+}\pi^{-}J/\psi$ and Observation of a Charged Charmoniumlike State at Belle. *Phys. Rev. Lett.* **2013**, *110*, 252002; Erratum in *Phys. Rev. Lett.* **2013**, *111*, 019901. [CrossRef]
15. Xiao, T.; Dobbs, S.; Tomaradze, A.; Seth, K.K. Observation of the Charged Hadron $Z_c^{\pm}(3900)$ and Evidence for the Neutral $Z_c^{0}(3900)$ in $e^{+}e^{-} \to \pi\pi J/\psi$ at $\sqrt{s} = 4170$ MeV. *Phys. Lett. B* **2013**, *727*, 366–370. [CrossRef]
16. BESIII Collaboration. Observation of $Z_c(3900)^{0}$ in $e^{+}e^{-} \to \pi^{0}\pi^{0}J/\psi$. *Phys. Rev. Lett.* **2015**, *115*, 112003. [CrossRef]
17. BESIII Collaboration. Observation of a charged $(D\bar{D}^{*})^{\pm}$ mass peak in $e^{+}e^{-} \to \pi D\bar{D}^{*}$ at $\sqrt{s} = 4.26$ GeV. *Phys. Rev. Lett.* **2014**, *112*, 022001. [CrossRef] [PubMed]
18. BESIII Collaboration. Confirmation of a charged charmoniumlike state $Z_c(3885)^{\mp}$ in $e^{+}e^{-} \to \pi^{\pm}(D\bar{D}^{*})^{\mp}$ with double D tag. *Phys. Rev. D* **2015**, *92*, 092006. [CrossRef]
19. BESIII Collaboration. Observation of a Charged Charmoniumlike Structure $Z_c(4020)$ and Search for the $Z_c(3900)$ in $e^{+}e^{-} \to \pi^{+}\pi^{-}h_c$. *Phys. Rev. Lett.* **2013**, *111*, 242001. [CrossRef]
20. BESIII Collaboration. Observation of $e^{+}e^{-} \to \pi^{0}\pi^{0}h_c$ and a Neutral Charmoniumlike Structure $Z_c(4020)^{0}$ *Phys. Rev. Lett.* **2014**, *113*, 212002. [CrossRef]
21. BESIII Collaboration. Observation of a charged charmoniumlike structure in $e^{+}e^{-} \to (D^{*}\bar{D}^{*})^{\pm}\pi^{\mp}$ at $\sqrt{s} = 4.26$GeV. *Phys. Rev. Lett.* **2014** *112*, 132001. [CrossRef]
22. BESIII Collaboration. Observation of a neutral charmoniumlike state $Z_c(4025)^{0}$ in $e^{+}e^{-} \to (D^{*}\bar{D}^{*})^{0}\pi^{0}$. *Phys. Rev. Lett.* **2015**, *115*, 182002. [CrossRef] [PubMed]
23. BESIII Collaboration. Observation of a Near-Threshold Structure in the K^{+} Recoil-Mass Spectra in $e^{+}e^{-} \to K^{+}(D_s^{-}D^{*0} + D_s^{*-}D^{0})$. *Phys. Rev. Lett.* **2021**, *126*, 102001. [CrossRef] [PubMed]
24. LHCb Collaboration. Observation of New Resonances Decaying to $J/\psi K^{+}$ and $J/\psi\phi$. *Phys. Rev. Lett.* **2021**, *127*, 082001. [CrossRef] [PubMed]
25. Belle Collaboration. Observation of two charged bottomonium-like resonances in Y(5S) decays. *Phys. Rev. Lett.* **2012**, *108*, 122001. [CrossRef] [PubMed]
26. Maiani, L.; Piccinini, F.; Polosa, A.D.; Riquer, V. Diquark-antidiquarks with hidden or open charm and the nature of X(3872). *Phys. Rev. D* **2005**, **71**, 014028. [CrossRef]

27. Ebert, D.; Faustov, R.N.; Galkin, V.O.; Lucha, W. Masses of tetraquarks with two heavy quarks in the relativistic quark model. *Phys. Rev. D* **2007**, *76*, 114015. [CrossRef]
28. Anwar, M.N.; Ferretti, J.; Santopinto, E. Spectroscopy of the hidden-charm $[qc][\bar{q}\bar{c}]$ and $[sc][\bar{s}\bar{c}]$ tetraquarks in the relativized diquark model. *Phys. Rev. D* **2018**, *98*, 094015. [CrossRef]
29. Tornqvist, N.A. From the deuteron to deusons, an analysis of deuteron-like meson meson bound states. *Z. Phys. C* **1994**, *61*, 525–537. [CrossRef]
30. Tornqvist, N.A. Isospin breaking of the narrow charmonium state of Belle at 3872 MeV as a deuson. *Phys. Lett. B* **2004**, *590*, 209–215. [CrossRef]
31. Swanson, E.S. Short range structure in the X(3872). *Phys. Lett. B* **2004**, *588*, 189–195. [CrossRef]
32. Hanhart, C.; Kalashnikova, Y.S.; Kudryavtsev, A.E.; Nefediev, A.V. Reconciling the X(3872) with the near-threshold enhancement in the $D^0\bar{D}^{*0}$ final state. *Phys. Rev. D* **2007**, *76*, 034007. [CrossRef]
33. LHCb Collaboration. Observation of structure in the J/ψ-pair mass spectrum. *Sci. Bull.* **2020**, *65*, 1983–1993. [CrossRef] [PubMed]
34. CMS Collaboration. New Structures in the J/ψJ/ψ Mass Spectrum in Proton-Proton Collisions at s = 13 TeV. *Phys. Rev. Lett.* **2024**, *132*, 111901. [CrossRef]
35. ATLAS Collaboration. Observation of an Excess of Dicharmonium Events in the Four-Muon Final State with the ATLAS Detector. *Phys. Rev. Lett.* **2023**, *131*, 151902. [CrossRef]
36. ANDY Collaboration. Observation of Feynman scaling violations and evidence for a new resonance at RHIC. *arXiv* **2019**, arXiv:1909.03124.
37. Chen, H.X.; Chen, W.; Liu, X.; Zhu, S.L. The hidden-charm pentaquark and tetraquark states. *Phys. Rept.* **2016**, *639*, 1–121. [CrossRef]
38. Esposito, A.; Pilloni, A.; Polosa, A.D. Multiquark Resonances. *Phys. Rept.* **2017**, *668*, 1–97. [CrossRef]
39. Lebed, R.F.; Mitchell, R.E.; Swanson, E.S. Heavy-Quark QCD Exotica. *Prog. Part. Nucl. Phys.* **2017**, *93*, 143–194. [CrossRef]
40. Ali, A.; Lange, J.S.; Stone, S. Exotics: Heavy Pentaquarks and Tetraquarks. *Prog. Part. Nucl. Phys.* **2017**, *97*, 123–198. [CrossRef]
41. Olsen, S.L.; Skwarnicki, T.; Zieminska, D. Nonstandard heavy mesons and baryons: Experimental evidence. *Rev. Mod. Phys.* **2018**, *90*, 015003. [CrossRef]
42. Guo, F.K.; Hanhart, C.; Meißner, U.G.; Wang, Q.; Zhao, Q.; Zou, B.S. Hadronic molecules. *Rev. Mod. Phys.* **2018**, *90*, 015004; Erratum in *Rev. Mod. Phys.* **2022**, *94*, 029901. [CrossRef]
43. Yuan, C.Z. The XYZ states revisited. *Int. J. Mod. Phys. A* **2018**, *33*, 1830018. [CrossRef]
44. Brambilla, N.; Eidelman, S.; Hanhart, C.; Nefediev, A.; Shen, C.P.; Thomas, C.E.; Vairo, A.; Yuan, C.Z. The XYZ states: Experimental and theoretical status and perspectives. *Phys. Rept.* **2020**, *873*, 1–154. [CrossRef]
45. Liu, Y.R.; Chen, H.X.; Chen, W.; Liu, X.; Zhu, S.L. Pentaquark and Tetraquark states. *Prog. Part. Nucl. Phys.* **2019**, *107*, 237–320. [CrossRef]
46. Chen, H.X.; Chen, W.; Liu, X.; Liu, Y.R.; Zhu, S.L. An updated review of the new hadron states. *Rept. Prog. Phys.* **2023**, *86*, 026201. [CrossRef]
47. Liu, M.Z.; Pan, Y.W.; Liu, Z.W.; Wu, T.W.; Lu, J.X.; Geng, L.S. Three ways to decipher the nature of exotic hadrons: Multiplets, three-body hadronic molecules, and correlation functions. *Phys. Rept.* **2025**, *1108*, 1–108.
48. D0 Collaboration. Evidence for a $B_s^0\pi^\pm$ state. *Phys. Rev. Lett.* **2016**, *117*, 022003. [CrossRef]
49. LHCb Collaboration. Search for Structure in the $B_s^0\pi^\pm$ Invariant Mass Spectrum. *Phys. Rev. Lett.* **2016**, *117*, 152003. [CrossRef]
50. LHCb Collaboration. A model-independent study of resonant structure in $B^+ \to D^+D^-K^+$ decays. *Phys. Rev. Lett.* **2020**, *125*, 242001. [CrossRef]
51. LHCb Collaboration. Amplitude analysis of the $B^+ \to D^+D^-K^+$ decay. *Phys. Rev. D* **2020**, *102*, 112003. [CrossRef]
52. LHCb Collaboration. First Observation of a Doubly Charged Tetraquark and Its Neutral Partner. *Phys. Rev. Lett.* **2023**, *131*, 041902. [CrossRef] [PubMed]
53. LHCb Collaboration. Amplitude analysis of $B^0 \to \bar{D}^0D_s^+\pi^-$ and $B^+ \to D^-D_s^+\pi^+$ decays. *Phys. Rev. D* **2023**, *108*, 012017. [CrossRef]
54. LHCb Collaboration. Observation of an exotic narrow doubly charmed tetraquark. *Nat. Phys.* **2022**, *18*, 751–754. [CrossRef]
55. LHCb Collaboration. Study of the doubly charmed tetraquark T_{cc}^+. *Nat. Commun.* **2022**, *13*, 3351. [CrossRef] [PubMed]
56. Liu, W.Y.; Chen, H.X. Fully-heavy hadronic molecules $B_c^{(*)+}B_c^{(*)-}$ bound by fully-heavy mesons. *arXiv* **2023**, arXiv:2312.11212.
57. Liu, W.Y.; Chen, H.X. Hadronic molecules with four charm or beauty quarks. *arXiv* **2024**, arXiv:2405.14404.
58. Cui, Y.; Chen, X.L.; Deng, W.Z.; Zhu, S.L. The Possible Heavy Tetraquarks $qQ\bar{q}\bar{Q}$, $qq\bar{Q}\bar{Q}$ and $qQ\bar{Q}\bar{Q}$. *High Energy Phys. Nucl. Phys.* **2007**, *31*, 7–13.
59. Chen, K.; Liu, X.; Wu, J.; Liu, Y.R.; Zhu, S.L. Triply heavy tetraquark states with the $QQ\bar{Q}\bar{q}$ configuration. *Eur. Phys. J. A* **2017**, *53*, 5. [CrossRef]
60. Weng, X.Z.; Deng, W.Z.; Zhu, S.L. Triply heavy tetraquark states. *Phys. Rev. D* **2022**, *105*, 034026. [CrossRef]

61. Junnarkar, P.; Mathur, N.; Padmanath, M. Study of doubly heavy tetraquarks in Lattice QCD. *Phys. Rev. D* **2019**, *99*, 034507. [CrossRef]
62. Hudspith, R.J.; Colquhoun, B.; Francis, A.; Lewis, R.; Maltman, K. A lattice investigation of exotic tetraquark channels. *Phys. Rev. D* **2020**, *102*, 114506. [CrossRef]
63. Jiang, J.F.; Chen, W.; Zhu, S.L. Triply heavy $QQ\bar{Q}\bar{q}$ tetraquark states. *Phys. Rev. D* **2017**, *96*, 094022. [CrossRef]
64. Zhang, W.S.; Tang, L. Investigating triply heavy tetraquark states through QCD sum rules. *arXiv* **2024**, arXiv:2412.11531.
65. Liu, Y.; Nowak, M.A.; Zahed, I. Heavy Holographic Exotics: Tetraquarks as Efimov States. *Phys. Rev. D* **2019**, *100*, 126023. [CrossRef]
66. Mutuk, H. Flavor exotic triply-heavy tetraquark states in AdS/QCD potential. *Eur. Phys. J. C* **2023**, *83*, 358. [CrossRef]
67. Zhu, Z.H.; Zhang, W.X.; Jia, D. Triply heavy tetraquark states: Masses and other properties. *Eur. Phys. J. C* **2024**, *84*, 344. [CrossRef]
68. Lü, Q.F.; Chen, D.Y.; Dong, Y.B.; Santopinto, E. Triply-heavy tetraquarks in an extended relativized quark model. *Phys. Rev. D* **2021**, *104*, 054026. [CrossRef]
69. Meng, L.; Chen, Y.K.; Ma, Y.; Zhu, S.L. Tetraquark bound states in constituent quark models: Benchmark test calculations. *Phys. Rev. D* **2023**, *108*, 114016. [CrossRef]
70. Liu, X.; Tan, Y.; Chen, D.; Huang, H.; Ping, J. Possible triply heavy tetraquark states in a chiral quark model. *Phys. Rev. D* **2023**, *107*, 054019. [CrossRef]
71. Yang, G.; Ping, J.; Segovia, J. Triply charm and bottom tetraquarks in a constituent quark model. *Phys. Rev. D* **2024**, *110*, 054036 . [CrossRef]
72. Xing, Y. Weak decays of triply heavy tetraquarks $bc\bar{b}\bar{q}$. *Eur. Phys. J. C* **2020**, *80*, 57. [CrossRef]
73. Cheng, J.B.; Li, S.Y.; Liu, Y.R.; Liu, Y.N.; Si, Z.G.; Yao, T. Spectrum and rearrangement decays of tetraquark states with four different flavors. *Phys. Rev. D* **2020**, *101*, 114017. [CrossRef]
74. Wu, J.; Liu, X.; Liu, Y.R.; Zhu, S.L. Systematic studies of charmonium-, bottomonium-, and B_c-like tetraquark states. *Phys. Rev. D* **2019**, *99*, 014037. [CrossRef]
75. Li, S.Y.; Liu, Y.R.; Man, Z.L.; Si, Z.G.; Wu, J. $X(3960)$, $X_0(4140)$, and other compact $c\bar{c}s\bar{s}$ states. *Chin. Phys. C* **2024**, *48*, 063109. [CrossRef]
76. Li, S.Y.; Liu, Y.R.; Man, Z.L.; Si, Z.G.; Wu, J. Doubly heavy tetraquark states in a mass splitting model. *Phys. Rev. D* **2024**, *110*, 094044. [CrossRef]
77. CDF Collaboration. Observation of the $Y(4140)$ Structure in the $J/\psi\phi$ Mass Spectrum in $B^{\pm} \to J/\psi\phi K^{\pm}$ Decays. *Mod. Phys. Lett. A* **2017**, *32*, 1750139. [CrossRef]
78. Wu, J.; Liu, Y.R.; Chen, K.; Liu, X.; Zhu, S.L. $X(4140)$, $X(4270)$, $X(4500)$ and $X(4700)$ and their $cs\bar{c}\bar{s}$ tetraquark partners. *Phys. Rev. D* **2016**, *94*, 094031. [CrossRef]
79. Stancu, F. Can Y(4140) be a $c\bar{c}s\bar{s}$ tetraquark? *J. Phys. G* **2010**, *37*, 075017; Erratum in *J. Phys. G* **2019**, *46*, 019501. [CrossRef]
80. Cheng, J.B.; Liu, Y.R. $P_c(4457)^+$, $P_c(4440)^+$, and $P_c(4312)^+$: Molecules or compact pentaquarks? *Phys. Rev. D* **2019**, *100*, 054002. [CrossRef]
81. Li, S.Y.; Liu, Y.R.; Man, Z.L.; Si, Z.G.; Wu, J. Hidden-charm pentaquark states in a mass splitting model. *Phys. Rev. D* **2023**, *108*, 056015. [CrossRef]
82. Particle Data Group. Review of Particle Physics. *Prog. Theor. Exp. Phys.* **2022**, *2022*, 083C01. [CrossRef]
83. Zhang, J.; Yi K., on behalf of the CMS Collaboration. Recent CMS results on exotic resonances. *Proc. Sci.* **2022**, *ICHEP2022*, 775. [CrossRef]
84. Wu, J.; Liu, Y.R.; Chen, K.; Liu, X.; Zhu, S.L. Hidden-charm pentaquarks and their hidden-bottom and B_c-like partner states. *Phys. Rev. D* **2017**, *95*, 034002. [CrossRef]
85. Li, S.Y.; Liu, Y.R.; Liu, Y.N.; Si, Z.G.; Wu, J. Pentaquark states with the $QQQq\bar{q}$ configuration in a simple model. *Eur. Phys. J. C* **2019** *79*, 87. [CrossRef]
86. Lü, Q.F.; Dong, Y.B. X(4140) , X(4274) , X(4500) , and X(4700) in the relativized quark model. *Phys. Rev. C* **2016**, *94*, 074007. [CrossRef]
87. Lebed, R.F.; Polosa, A.D. $\chi_{c0}(3915)$ As the Lightest $c\bar{c}s\bar{s}$ State. *Phys. Rev. C* **2016**, *93*, 094024. . [CrossRef]
88. Yang, Y.; Ping, J. Investigation of $cs\bar{c}\bar{s}$ tetraquark in the chiral quark model. *Phys. Rev. C* **2019**, *99*, 094032. [CrossRef]
89. Bokade, C.A.; Bhaghyesh. Charmonium: Conventional and XYZ States in a Relativistic Screened Potential Model. *arXiv* **2024**, arXiv:2408.06759.
90. Barnes, T.; Black, N.; Swanson, E.S. Meson meson scattering in the quark model: Spin dependence and exotic channels. *Phys. Rev. C* **2001**, *63*, 025204. [CrossRef]